Sedimentary and sea level changes during glacial cycles and their control on glacimarine facies architecture

G.S. BOULTON

Department of Geology and Geophysics, Grant Institute, Kings Buildings, University of Edinburgh, West Mains Road, Edinburgh EH9 3JW, UK

Abstract: In part 1 a simple sedimentation model is presented in which subglacial ice-contact, proglacial ice-contact, inner and outer proximal, and distal glacimarine zones are distinguished. In these, facies associations are controlled by: (a) distance from the glacier and the diffusion of glacially-derived water masses and their suspended sedimentary (including berg-transported) debris into nearby oceanic waters; (b) the form and depth of the sea bed, and its position in relation to the continental margin (which help determine water mass character and tidal, wave-driven and geostrophic currents and the stability of sea-bottom sediments).

In part 2 a model of eustatic/isostatic sea level change in the vicinity of a generic ice sheet through a whole glacial cycle is developed. The sedimentation model from part 1 is linked to the sea level model to predict patterns of marine sedimentation near to an ice sheet through a glacial cycle, in inner shelf, outer shelf and continental slope environments.

Comparisons are made between theoretical models and observed patterns of glacimarine facies architecture produced during the last glaciation of Britain, continental Europe and Spitsbergen. The phase relationship between local ice sheet advance and retreat and that of the Laurentide ice sheet, the principal determinant of global eustatic change, is a major determinant of large scale sedimentation patterns.

Cycles of ice sheet expansion and decay produce characteristic three-dimensional patterns of glacimarine facies and relationships to glaciterrestrial and non-glacial sediments. Repetitive styles of facies architecture reflect the intimate relationships between many of the principal controls on sedimentation rate and sediment character during glacial cycles. They are a response to interactions between four coupled phenomena: the geometry of the crust; the spatial and temporal pattern of expansion and decay of the ice sheet (and its phase relation to the global glaci-eustatic cycle); isostatic response of the crust; and patterns of ocean circulation.

This article explores the consequences of these interactions for facies architecture. It does so in two parts. The first discusses the instantaneous spatial organization of facies in relation to the position of the glacier, the form of the depositional surface and ocean–water circulation. The second discusses the influence of ice sheet expansion and decay and the associated relative sea level changes in limiting and displacing facies zones and determining their overall geometry.

The large scale three-dimensional architecture of sediment sequences is a reflection of the organization of sedimentary environments in space and time. Each major environment is characterized by sets of interacting processes which produce repetitive associations of lithofacies. Individual lithofacies are not described in this paper, but rather the sets of processes typical of each environment and the genetic sediment types which they produce.

Part 1: Glacimarine facies distributions in space: (a) the ice-contact zone

Ice contact sediments and landforms in glacimarine environments comprise: (a) those which form subglacially and which are progressively exposed on the sea floor during glacier retreat (though not formed in a marine environment, they are discussed here as they form the substratum for many glacimarine sequences); (b) those which form at the glacier front.

Subglacial sediment and landforms

There is no fundamental reason why subglacial sedimentary processes should be different in kind beneath glaciers terminating in water and those terminating on land. The buoyant forces which influence the terminal zones of the former can merely be regarded as contributing to the

From DOWDESWELL, J. A. & SCOURSE, J. D. (eds), 1990, *Glacimarine Environments: Processes and Sediments*. Geological Society Special Publication No 53, pp 15–52.

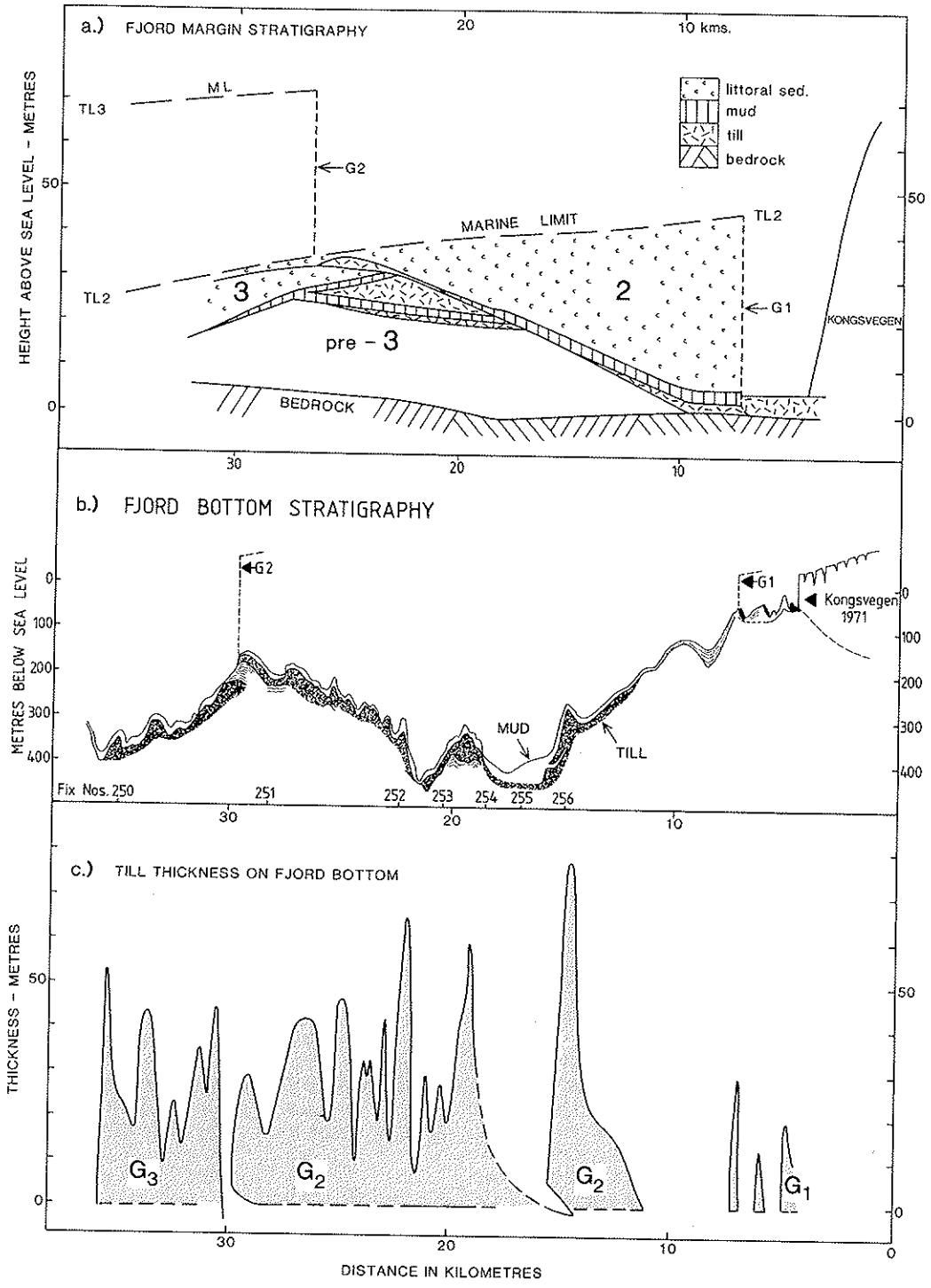

Fig. 1. Comparison of the thickness and character of the mid-fjord and fjord margin sedimentary sequences in Kongsfjorden, Spitsbergen (see Fig. 11). (a) The sequence exposed above sea level on the northern shore of Kongsfjorden. Numbers 1–3 represent glacioisostatic facies cycles as shown in Fig. 26. G1, G2 show glacier maximum positions in cycles 1 and 2. TL_2 and TL_3 show transgression limits for cycles 2 and 3. Modern sea level is the transgression limit for cycle 1. (b) Fjord bottom stratigraphy based on interpretations of sparker survey (1971). (c) Thickness of fjord bottom till produced by glacial events G1, G2 and G3 along the same line as b.

diminution of subglacial effective pressures towards the terminus in much the same way as occurs beneath the wedge-shaped termini of glaciers ending on land. We therefore expect flutes (see Solheim *et al.* 1990) drumlins and eskers to form beneath marine-based glaciers as they do on land.

There is a frequent contrast between the thickness of the tills produced by marine based glaciers compared with those produced by terrestrial glaciers. For instance, in Spitsbergen during the last century, the glacier Sefströmbreen advanced rapidly over an arm of the sea and onto an island, Cora Island, where it deposited up to 10–20 m of deformation till consisting of remoulded marine mud (De Geer 1910; Lamplugh 1911; Boulton & Van der Meer 1989). Similarly Kongsvegen, also in Spitsbergen, advanced over the eastern Løven islands (Elverhøi *et al.* 1983) and plastered on to it over 5 m of remoulded marine mud, which seismic records just offshore show to be up to 25 m in thickness (Fig. 1). Entirely terrestrially-derived tills, deposited on land from both these episodes, do not exceed 1–2 m in thickness. I suggest that a glacier flowing over mud-dominated glacimarine sediments, through which drainage will be poor, will induce high pore-water pressures in them and through deformation, remould substantial thicknesses of marine mud into deformation till. Further glacially-transported debris may be added through release of englacial debris as a consequence of melting of basal ice. On the land margin, however, coarse littoral deposits resulting from the previous glacio-isostatic cycle will tend to be more resistant to glacier-induced forces and also facilitate subglacial drainage and pore water pressure dissipation so that sediment remoulding will not be such an effective mechanism of till generation (Fig. 1- Boulton & Jones, 1979; Boulton, 1987).

Where glaciers flow into marine environments, the buoyant force of the water mass, and soft, easily-deformable subglacial sediments tend to reduce basal frictional resistance, which is conducive to a fast flow typical of ice streams, which tend to draw down ice domes in the hinterland. In many cases, such areas are prone to surging behaviour (cf. Elverhøi *et al.* 1983) and develop large longitudinal tensile stresses which cause extensive crevassing. Soft subglacial sediment is intruded into crevasses, and if the glacier tongue stagnates, as is generally the case at the end of a surge, the intruded till ridges survive after ice melting and form reticulate patterns on the sea floor. Figure 2 shows the pattern of crevasse-intruded ridges which survived after the Sefströmbreen surge of 1896. This process was first identified by de Geer (1910) and has been amplified by Lamplugh (1911), Gripp (1929), Solheim & Pfirman (1985) and others.

Proglacial sediments and land forms

Subglacial and englacial streams draining a glacier are subject to a much more dramatic check on their velocities when they enter the sea than when they drain from a terrestrial ice margin. Although suspended sediment concentrations may make some meltwater dense enough to form underflows which retain bed contact, most rises to the sea surface to form turbid brackish-water plumes (Fig. 3). Thus, coarse, fluvially-transported sediment, tends to be much more restricted to the immediate ice margin in glaciers flowing into the sea compared

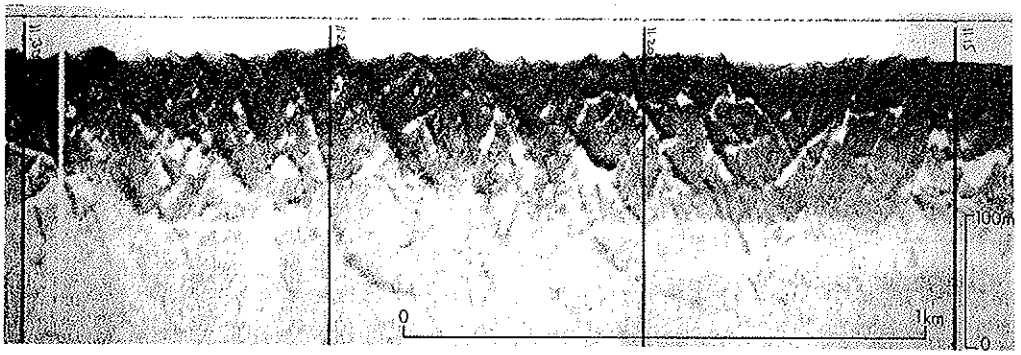

Fig. 2. Transit sonar image showing glacially-overridden glacimarine sediments which have been pressed-up into crevasses which formed during the surge of Sefströmbreen, Spitsbergen. The sediments (up to 15 m thick) were sheared along beneath the glacier during the surge.

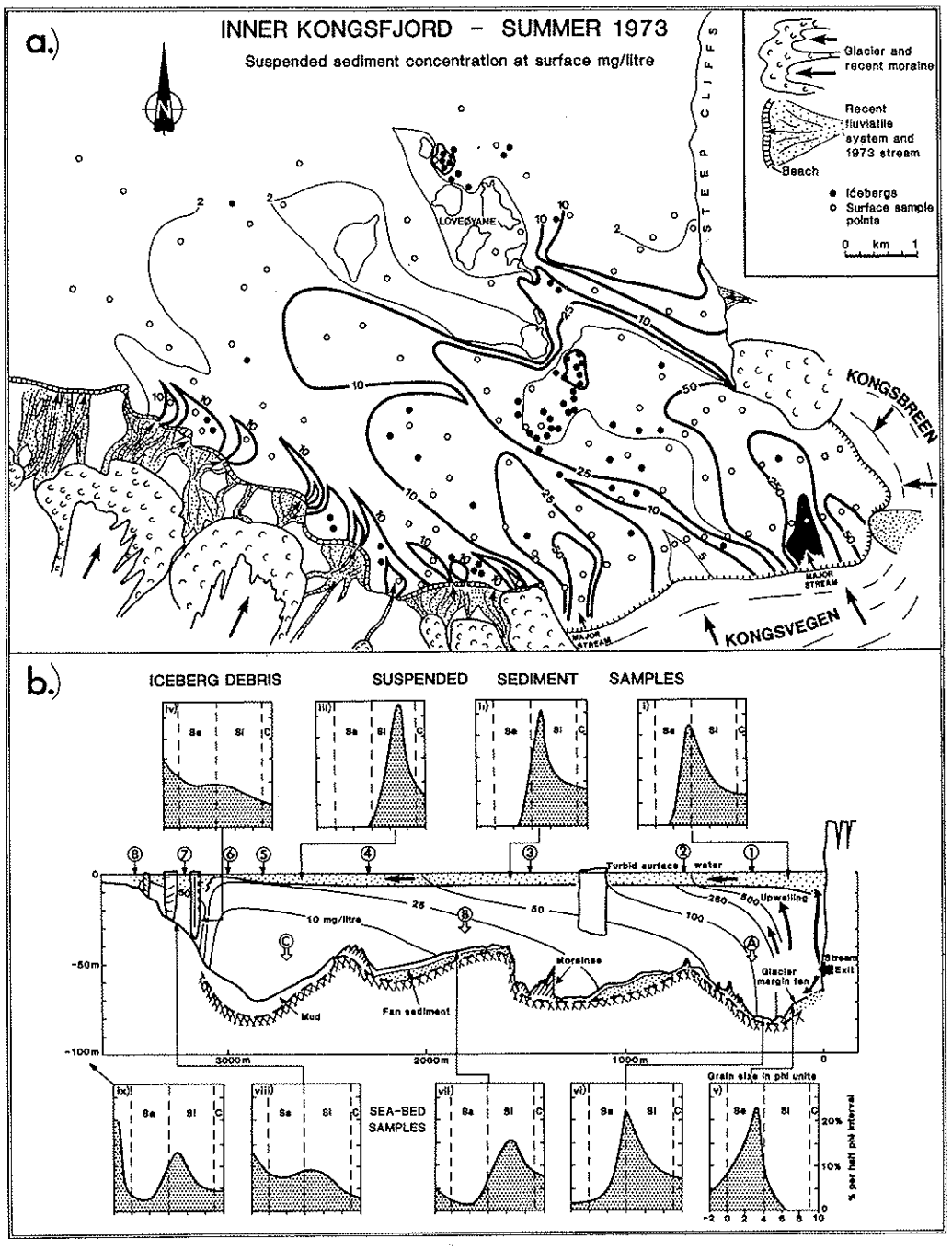

Fig. 3. (a) Suspended sediment concentrations in surface waters and the location of large icebergs in the proglacial area of Kongsvegen, Spitsbergen (Fig. 1). Measurements were taken from four boats during a two-hour period spanning high tide at a time of negligible surface wind (July 23, 1973), using a light attenuation metre calibrated by water samples. Inter-station turbidity contours were interpolated from photographs taken from nearby mountain peaks. Suspended sediment is largely derived from two dominant meltwater rivers which emerge from ice-front tunnels. (b) Section in the same area normal to the glacier front, showing fjord bottom geology, suspended sediment concentrations and grain-size distribution of sediment on the bed, in the water column and collected in sediment traps. A, B and C show the location of sediment traps (point of arrow). Fjord bottom geology (see Boulton 1986) was determined by sparker profiling and core and grab sampling. Suspended sediment concentrations were measured from profiles using a light attenuation metre at the same time as the measurements in (a). Sediment traps were emplaced for 10 days.

with their terrestrial counterparts. The coarse-grained submarine fans which they form thus tend to hug the ice margin (Powell 1981). The location of these fans is determined by the temporal pattern of ice front fluctuation and the location and stability of meltwater stream outlets (Boulton 1986). If the ice front undergoes a major readvance, or a winter readvance during general retreat, push-moraines tend to form. The origin and structure of these features has been described by Birnie (1977) for glacier margins on land, and by Boulton (1986) for marine margins.

Figure 4 shows a schematic diagram which illustrates the assemblage of ice-contact forms produced by a glacier draining into a fjord.

Fan bodies which accumulate at the margin of Kongsvegen are up to 15 m in thickness, and 300 m across (Fig. 3b). The point of entry into the fjord of the streams which feed them is extremely unstable, partially due to falling seracs which must block tunnel mouths. As a consequence fan sediment masses produced by a single unstable stream may extend for several hundred metres across the glacier front. If several streams come into the fjord, we should expect a series of transversely-oriented fan ridges from each stream, but with similar longitudinal spacings, as discussed by Boulton (1986).

If the grounding line does not coincide with the ice front, as in the case of an ice shelf, we may expect subglacial deltas to develop from sediment transported at the glacier/bed interface. This sediment may be water-transported or ice-transported. The bulk of water transport is likely to occur as channelled flows which discharge sediment from specific points at the grounding line to produce fans or deltas. Disseminated flow is likely to discharge a much smaller volume of water or sediment, either by sheet-flow at an ice bedrock interface (Weertman 1972) or as an intergranular flow through a subglacial sediment (Boulton & Hindmarsh 1987).

Ice-transported detritus may be englacial or in a subglacial deforming layer. A glacier moving over a bedrock surface with only an englacial load is unlikely to transport enough material to supply a significant delta, but a deforming subglacial bed may (Alley *et al.*

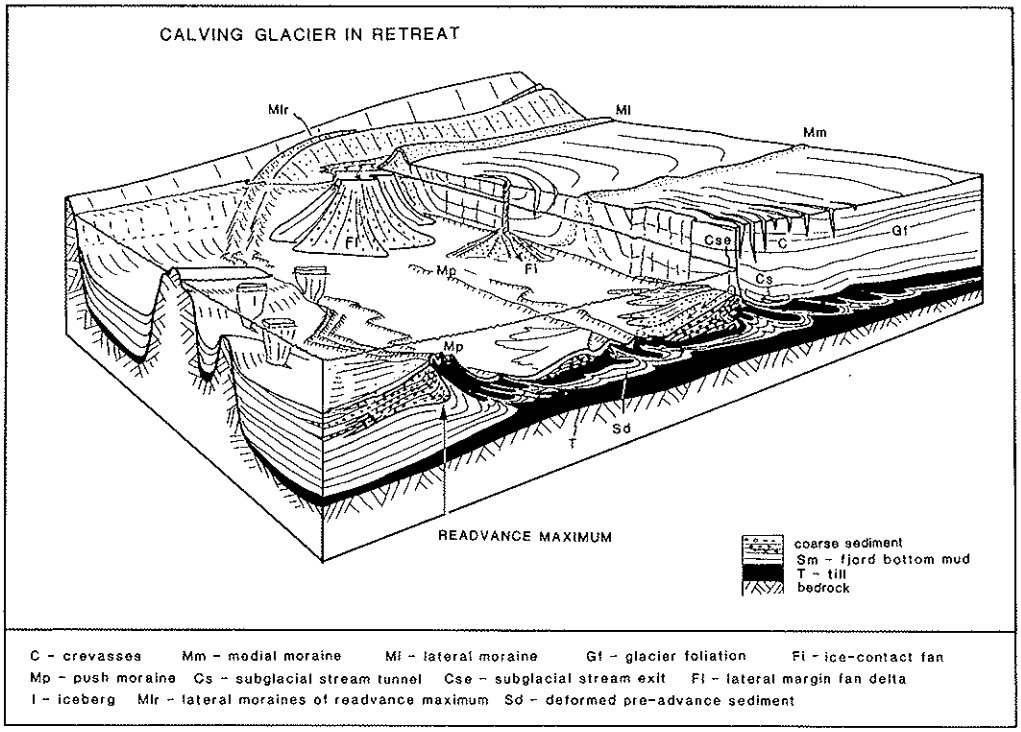

Fig. 4. Schematic diagram showing the principal sea-bed features in the proglacial area of a calving glacier, and the underlying sedimentary sequences.

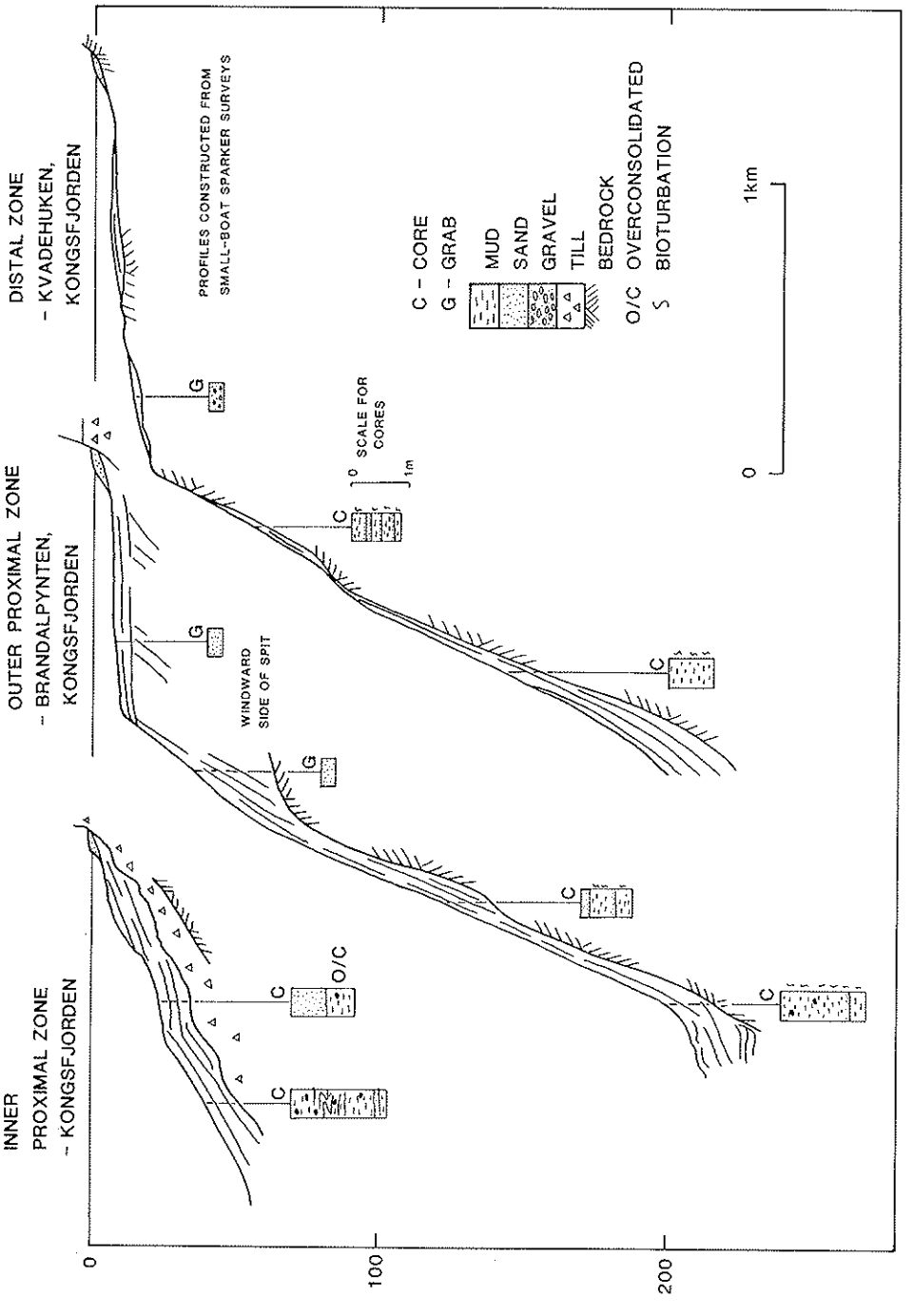

Fig. 5. Shore-face facies in a variety of proximal and distal locations.

1987), producing a two-dimensional deltaic feature all along the grounding line, provided that the bed slopes steeply enough (Fig. 6).

Sorting processes during flow and avalanching of this deformation till down the delta foresets will tend to produce stratification. Both two-dimensional *till-fed* and three-dimensional *stream-fed* deltas will respond similarly to changing sea level. If sea level is static, prograding foresets will build out, to which, in till-fed deltas, the deforming till mass will provide topsets (Fig. 6Ai). A sea level rise will cause retreat of the grounding line (Fig. 6Aii), but subsequent stabilization will cause development of a second prograding foreset/till topset couplet (Fig. 6Aiii). A sea level fall (Fig. 6Aiia) will tend to enhance development of a foreset/topset couplet at a lower level, caused by lowering of the base of the ice shelf. Where a glacier extends to the continental shelf edge, both till-fed and stream-fed deltas will tend to form at the shelf break in response to eustatic and isostatic changes in sea level (Fig. 6B).

King & Fader (1986) and King *et al.* (1987) have discussed possible subglacial processes at the shelf break through their seismostratigraphic studies of the Scotian and Mid-Norwegian shelves. They identify *till tongues* which interdigitate with glacimarine units at the shelf-break in response to changes in the position of the grounding line, in much the way shown in Fig. 6A. However, they believe that the melt-out process would be the principal source of sediment, either as till proximal to the grounding-line, or as a sediment deposited by settling through the water column distal to the grounding line. I would stress the potentially greater volumetric importance of shear transport and remoulding of subglacial sediments (Boulton & Jones 1979) as a source of till, and, in such a regime, the importance of slumping of the deformation till which is continuously discharged at

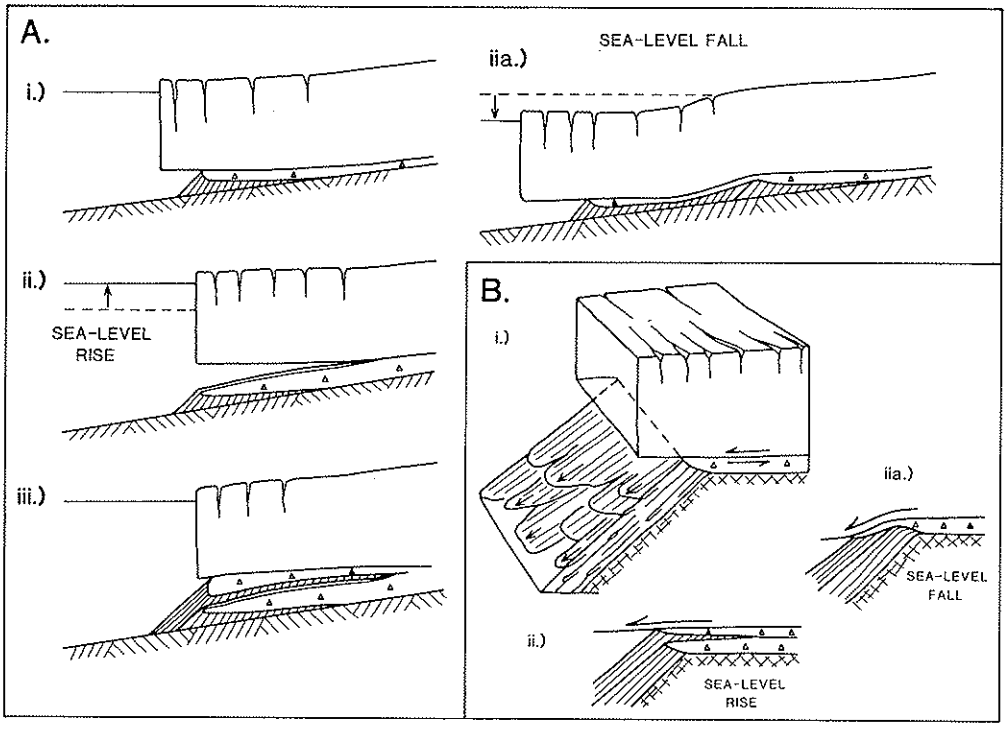

Fig. 6. Suggested sedimentary response of sub-ice shelf sediments to sea-level change. Note that deposits from suspension are omitted. (a) Sedimentation changes beneath an ice shelf on a continental shelf. i-ii-iii show the response to sea level rise, and i-iia show the response to sea level fall. (b) Sedimentation beneath an ice shelf whose grounding line occurs at the continental shelf edge. i-ii show the response to sea level rise and i-iia the response to sea-level fall. Till (assumed to form largely from shear-remoulded marine mud) is shown by triangles. Prograded foresets are shown which reflect the advance of the grounding line. Note how sea level rise leads to formation of two couplets.

the grounding line (cf. Alley *et al.* 1987). The deformation process does not require erosion of immediately subjacent materials. They may be derived from far up-glacier with deposition predominant in the terminal zone of the glacier (cf. Fig. 12).

(b) The proximal zone: inner shelf or inner fjord

The glacier proximal zone, rarely in excess of 10–20 km in width is dominated by an estuarine style of water circulation during the summer season. Large volumes of densely sediment-charged meltwater are discharged from glacier termini. This may reach the sea from meltwater rivers where the glacier terminates on land, or directly from tunnels in or beneath the ice where the glacier terminates in the sea. They give rise to surface plumes of brackish, turbid, glacier meltwaters containing large suspended sediment concentrations (Fig. 3a), and induce a thermohaline counter current at depth.

Very high rates of sedimentation from suspension have been reported in such zones. Elverhøi *et al.* (1983) report 50–100 mm a^{-1} at a distance of 10 km from Kongsvegen in Spitsbergen. Powell & Cowan (1986) report 150–3000 mg cm^2 day^{-1} within 1 km of the front of McBride Glacier in Alaska. Figure 7 shows the sedimentation rate(S) falls off logarithmically with distraps moored 5 m above the sea floor beyond the glacier Kongsvegen in Spitsbergen, plotted together with data from other sources. Sedimentation rate(S) falls off logarithmically with distance from the glacier so that:

$$S(\text{mm a}^{-1}) = \log^{-1}[100 - 1.33 \log(d-1)]$$

where d is the distance from the glacier in km. The proximal environments from which measurements were taken are in fjords, where bottom currents are relatively weak and sedimentation from suspension dominates, apart from in the glacier-margin zone of fan deposition (Fig. 4). However, even on open, stormy coastlines such as that of southern Iceland, which is fed by major meltwater rivers, and even though glaciers do not reach the sea, a mud-dominated proximal zone extends for some 10–20 km beyond the river mouths (Boulton *et al.* 1988).

It is possible to distinguish an Inner Proximal Zone where sedimentation rates are sufficiently high to inhibit benthic life, and bioturbation is rare, and an Outer Proximal Zone, where benthic life and bioturbation are common (Fig. 7b) (Farrow *et al.* 1983).

An intensive study of suspended sediment concentration, sedimentation rate and sediment granulometry near the front of the tidewater glacier Kongsvegen was undertaken in late July 1973. Measurements of surface water turbidity and turbidity/depth profiles were taken using light-attenuation metres (calibrated against samples) from four vessels over a two-hour period spanning a single high tide at a time of slight surface wind. Inter-station contours of surface turbidity (Fig. 3a) were interpolated from photographs taken from nearby mountain peaks. It shows sediment plumes emanating from two major ice front streams believed to debouch into the fjord near to the base of the ice cliff.

Sub-surface processes were inferred from the turbidity/depth profiles, three sediment traps anchored between 17 and 35 m above the sea bed over a 10-day period, grab and core samples, and sparker profiles (Fig. 3b). Powerful turbulence and a raised water surface near to the plume apex suggested strong stream upwelling (see Syvitski 1989). In this zone (i), sediment in the plume had a mode at the fine sand/silt boundary. Further from the glacier (ii), the mode became finer-grained with no further sand in the plume by 2 km from the glacier (iii). On the sea-bed, the distal part of the ice-front fan (v) was sand-dominated. Muds just beyond the fan margin (vi) showed a mode in the sand fraction, but this rapidly gave way to a silt mode (vii) further from the glacier.

The high rate of sedimentation from suspension in the inner proximal zone tends to overwhelm the iceberg-dropped component (Fig. 3b, vi and vii; Fig. 7b; Fig. 8a) whereas in the outer proximal zone the berg-dropped component becomes important (Fig. 3b, ix; Fig. 7b; Fig. 8b). Icebergs tend to ground and become stranded in shallow areas and it is here that clast-rich diamictons tend to be produced from a sediment-rain dominated by iceberg-derived debris (Figs 7b & 8c). High turbidity often characterizes this zone (Fig. 3b) and any differences between the grain-size distribution of debris collected from bergs and sediment on the sea floor (Fig. 3b, iv, viii) reflects such processes as current winnowing and extraneous sediment inputs. High rates of sedimentation near to the glacier front tend to produce underconsolidated muds (Fig. 7b). These tend to be unstable and may generate mass flows and secondary turbidites (Fig. 8d). Evidence for such processes is frequently seen in sediment cores in the inner proximal zone, though it is rare in the outer proximal zone, except where very high bed slopes occur.

The influence of seabed slopes can be seen

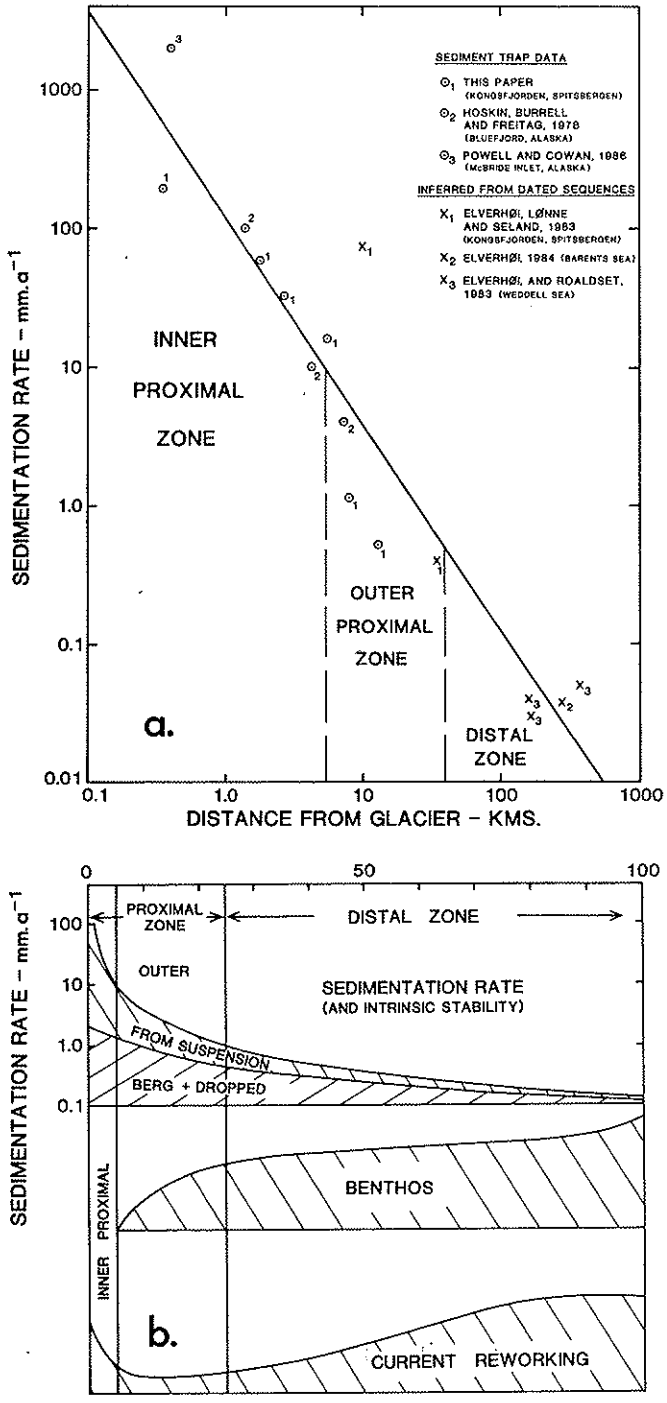

Fig. 7. (a) Relationships between sedimentation rate and distance from the glacier from a number of glacial environments. (b) Schematic diagram showing changing sediment properties with distance from the glacier.

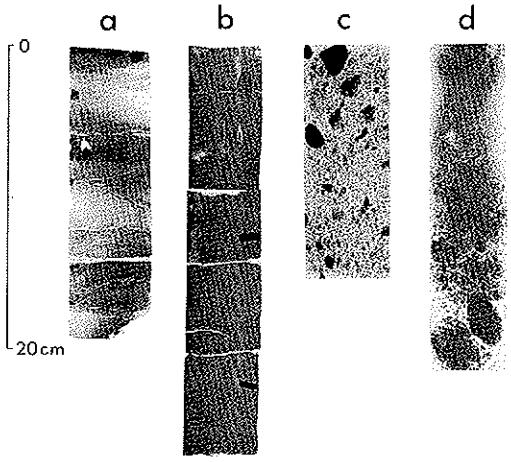

Fig. 8. X-rays from sediment cores in representative glacimarine environments. (a) Inner-proximal zone, Kongsfjord, Spitsbergen (site at 900 m, Fig. 3b). (b) Outer-proximal zone, Kongsfjord. A less silt-rich sediment showing bioturbation (150 m water depth). (c) Clast-rich diamicton from a shoal on which debris-rich icebergs ground, Kongsfjord (site at 3300 m, Fig. 3b). (d) Turbidite sequence generated by slumping from the flanks of Cambridge Fiord, Baffin Island (core CA4.2; see Fig. 9).

very clearly in the contrasts between fjord-bottom sedimentation in the outer proximal zone in many Spitsbergen and Baffin Island Fjords (Fig. 9). In the former, submarine fjord-margin slopes tend to be in the range of 5°−20°, and as a consequence there is very little evidence of gravity flows down the fjord margins. Sediments are draped over the underlying topography, and bioturbation is strong. In the latter, slopes are frequently in excess of 35−40°, and as a consequence, there is ample evidence of debris flows and secondary turbidite action. Sediments preferentially infill the fjord bottom and bioturbation is suppressed.

It is particularly important to understand sedimentary processes in the sublittoral zone as these are often important components of glacio-isostatically uplifted sequences seen on land. Figure 5 shows a series of sampled nearshore profiles from the inner proximal zone to the distal zone from the relatively sheltered environment of Kongsfjorden, Spitsbergen (including a profile from just beyond the fjord mouth). In the sheltered fjords there tend to be shallow (−5m) sub-beach platforms associated with normal wave activity and tidal fluctuations, below which, away from active sediment inputs, either bedrock is exposed (or lies at shallow depth beneath a thin sediment cover) or, in the case of inner Kongsfjorden, recently deposited till is currently being eroded. There is then a tendency for platform development at −20 to −30m which I interpret as wave base for storms, for wave height rarely exceeds 3−4 m in these sheltered environments (Syvitski *et al.* 1983). Moign (1965) reports evidence of strong sub-littoral erosion even in inner Kongsfjorden, Spitsbergen, down to a depth of 30 m below sea level, and on the open coast of Southern Iceland strong sub-littoral erosion has produced a 2 km wide bench at −20 m above the major prograding coastal sediment wedge built out during the Holocene by powerful meltwater rivers (Boulton *et al.* 1988). Thick mud units tend only to develop beneath this depth. Boulton *et al.* (1982) also concluded from the study of uplifted glacimarine sequences in Spitsbergen that −30 m was the upper level of mud accumulation.

At points of sediment input to the fjord basin, such as fan-deltas and spits, a coarse-grained sandy apron may descend to considerable depth (Fig. 5b) (e.g. Syvitski 1987; Boulton *et al.* 1985).

If we presume that the primary deposition rate of glacially-derived sediment from a fjord head glacier is a function of distance from the glacier source (Figs 3 & 7), the nature of shoreface sedimentation will depend upon the location of side inputs (Fig. 5) and the balance between primary sedimentation rate and rates of operation of different erosional agents. The latter are as follows.

Bottom currents. Strong shallow water currents can be associated with glacier-derived turbid surface plumes. The easternmost plume in Fig. 3a attains surface velocities of 6m s^{-1}, and is probably largely responsible for erosion of a prominent 200 m wide shelf at −23m in recently deposited till which was deposited on the fjord side during a neoglacial advance of Kongsvegen (fig. 5a).

Tidal currents may be particularly strong along the shoreface where fjords are constricted, and may reach to considerable depth. The profile in fig. 5b occurs at such a constriction. Sandy current winnowed units lying on shallow bedrock extend down to −70m.

Wave action. This is largely a function of exposure. In sheltered fjords, storm-wave

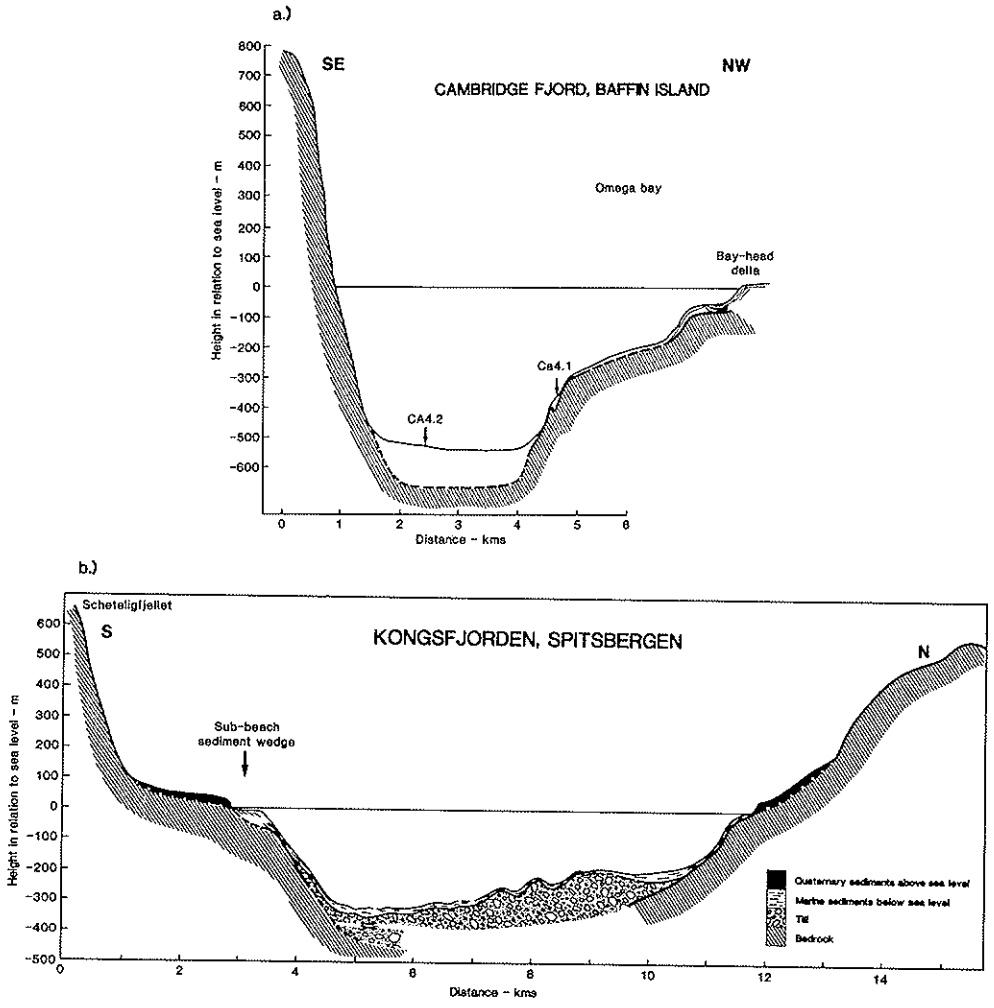

Fig. 9. Contrasts between (a) an "infill sequence" in Cambridge Fjord Baffin Island, where slumping from the steep margins (up to 40°) produces a flat-bottomed, slump and turbidite (Fig. 7d) infill sequence, and (b) a "draped-sequence" (Fig. 7b) in Kongsfjorden, Spitsbergen, where the fjord margin slopes are between 5° and 20°.

scoured platforms rarely extend to more than −20m.

Slumping and creep. The exceptionally high sedimentation rate in the inner proximal zone ensures that pore fluid pressure dissipation does not keep pace with sedimentation. Pore fluid contents 36% greater than in normally consolidated samples were found in muds at the base of 2.4 m long cores in flat bed areas of inner Kongsfjorden. As a consequence, sediment flow occurs on any significant slope in this zone, and sidescan sonographs show ubiquitous sediment creep features on the fjord sidewalls. However, although there is a strong tendency for an infill sequence to develop, high rates of sedimentation sustain a thin mud drape on the fjord walls (Fig. 5)

In the outer proximal zone, sedimentation rates are lower, sediment is more stable and draped sequences become the norm on gently sloping shore-faces. We thus expect a sequence resulting from glacier retreat to show a transition from infill to draped sequence as the inner proximal gives way to the outer proximal zone. Fig. 5b may show an example of this.

Iceberg disruption. Major sediment disruption can occur along tracks of iceberg dispersal (Barnes & Rearic 1985). Moreover small bergs aground in shallow water, rising and falling under storm wave action, may have a significant effect in eroding and reorganizing shallow shore platforms.

Benthonic life is also strongly controlled by shoreface processes (e.g. Dale *et al.* 1989). It is generally inhibited in the inner proximal zone by high rates of sedimentation, although shallow wave and current-scoured surfaces can be well colonised. In the outer proximal zone, there is a richer benthonic fauna below the level of wave and current scour.

(c) The distal zone: outer shelf or outer fjord

The distal sedimentary regime contrasts strongly with that in the proximal zone. Suspended sediment concentrations in the water column may be up to three orders of magnitude less than in the inner proximal zone (Fig. 7). Moreover, upwelling of deep water along the continental margin (Anderson *et al.* 1984; Jacobs, 1989) and/or strong long-shelf geostrophic currents (Boulton *et al.* 1988), coupled with the greater energy of long-waves associated with the outer shelf, generally ensure a more energetic sea bed environment than in the proximal zone. As a consequence, the distal zone tends to be one of sediment reworking down to considerable depth, erosion of earlier sediments and the formation of sandy and gravelly lag horizons.

Some deeper basins on outer shelves show evidence of mud sedimentation during the Holocence, although this rarely exceeds a net sedimentation rate of 10 cm/1000 years. On very broad shelves, such as the Barents Shelf, sediment reworking dominates near the shelf edge, where the oceanic influence is strongest, but in the inner part of the shelf, in water depths greater than 100 m, there has been net sedimentation of mud during the Holocene at rates of between 2 and 8 cm/1000 years (Elverhoi 1984). Enhanced nutrient supply in zones of upwelling sustains high rates of biological productivity and rich benthonic and planktonic floras and faunas, which contribute to important bioclastic horizons (Elverhoi 1984). A large proportion of the primary clastic sediment input to many outer shelf areas is of ice-rafted detritus (Orheim & Elverhoi 1981), although the input will vary strongly as iceberg tracks are strongly dependent on bathymetry and current and wind circulation.

The effects of some of these processes are shown in Fig. 10 of the Ross Sea, in Antarctica, and the western Spitsbergen continental shelf. There is strong upwelling along both margins producing strong currents and reworking at the shelf edge and a major bioclastic component in shelf-edge sediments. Away from the shelf edge, the depth of the Antarctic shelf is sufficient to inhibit reworking except on banks in less than 300 m of water (Anderson *et al.* 1984). In Spitsbergen strong long-shelf currents produce re-working on the mid-shelf, with strong sedimentation from turbid meltwater overflows in the innershelf (fjord) environment. It is possible that a similar effect may be produced in the Ross Sea from sub-ice shelf meltwater (Jacobs 1989). Sub-ice shelf melting in the Ross Sea ensures that icebergs from the ice shelf are debris-free, and thus that little berg-dropped material is deposited close to the ice shelf (Anderson *et al.* 1984). Berg-dropped material on the mid and outer shelf is derived from icebergs carried into the region from the west. In Spitsbergen, debris-transporting bergs are derived directly from the nearby ice margins as well as being transported from afar by the long-shelf current.

Most northern hemisphere glaciated shelves show a relatively simple geometry, of shallow planar banks of 100–200 m depth, crossed by glacially-eroded troughs which descend 300–400 m below sea level (Fig. 11).

On the Iceland shelf (Boulton *et al.* 1988) till is absent in the troughs and thick on their flanks and on the adjacent banks, apart from on the inner shelf where a moraine has been generated during a Late Weichselian glacier standstill or readvance. In Kongsfjorden and Isfjorden, on the western Spitsbergen Shelf, tills are absent in the troughs in the inner shelf, but do occur on the outer shelf where they thicken towards a shelf edge (Fig. 13a). In both cases however, till appears to occur across the whole shelf on the flanking banks, apart from in shallow-water zones where it has been removed by sub-littoral erosion.

A simple numerical model is used to help explain these patterns. When a glacier flows across a continental shelf showing linear, flow-parallel troughs and flanking banks, such as that of West Spitsbergen (Fig. 11) the trough depth will be inadequate to entirely channel a glacier extending near to the shelf edge, except in its terminal zone. As ice will be approximately 200 m thicker in the troughs than flanking banks, a greater driving stress will occur along the trough, leading to enhanced flow and a tendency

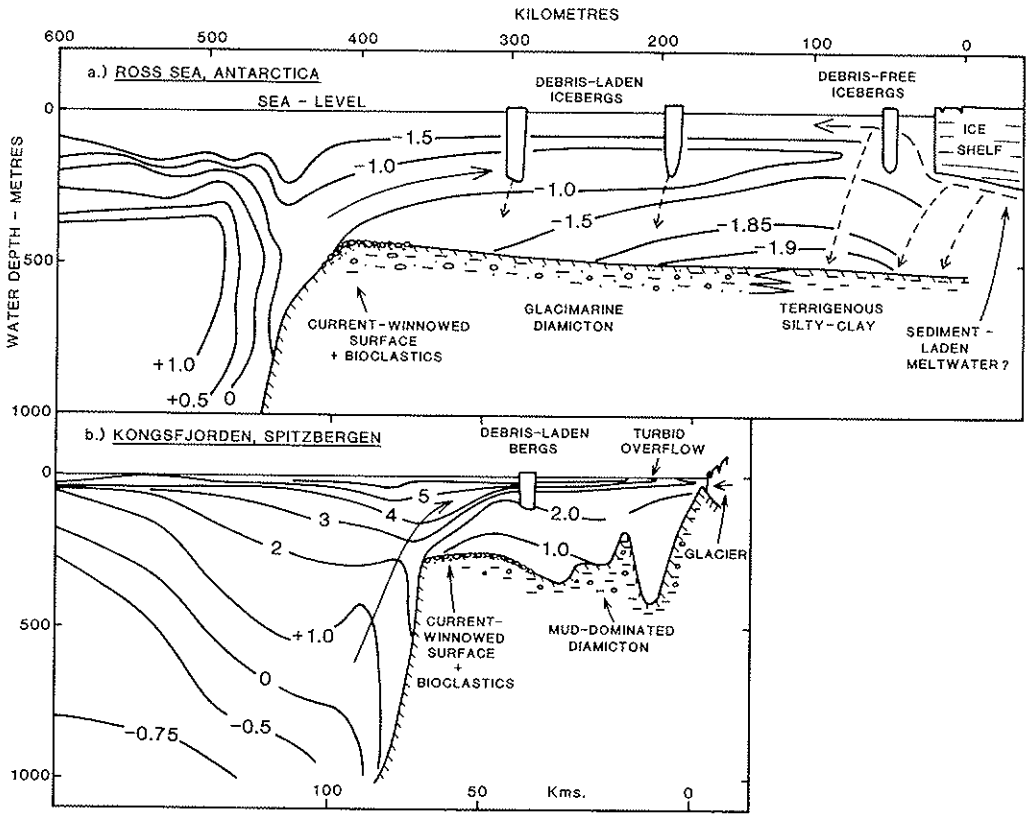

Fig. 10. Ocean thermal structure in summer in glacimarine environments from the glacier front across the continental shelf and into the deep ocean, showing the character of bottom sediments (thickness of the ornament does not represent sediment thickness). (a) Ross Sea, Antarctica (re-drawn from Anderson *et al.*, 1984). (b) Kongsfjorden and the west Spitsbergen continental shelf (NERC cruise *G.A. Reay* 1986).

for an ice stream to develop which draws down ice from the flanking banks.

At the basal boundary, we assume

$$U_b = \frac{\tau_b}{P_c^{\lambda}} \tag{1}$$

where U_b and τ_b are basal velocity and shear stress in the x-direction, and λ is a friction parameter (Morland *et al.* 1984).
For the ice stream

$$\tau_b = \rho g(H_1 + H_2) \sin \alpha. \tag{2}$$

For the banks adjacent to the ice stream

$$\tau_b = \rho g H_2 \sin \alpha \tag{3}$$

where H_1 is the depth of the trough below the bank's surface, H_2 is the ice thickness over the bank and α is the slope of the glacier surface. Longitudinal stresses and shear at the margins of the ice stream are ignored.
Discharge (Q_s) of the ice stream will be

$$Q_s = \frac{W\rho g(H_1 + H_2)^2 \sin \alpha}{P_c^{\lambda}} \tag{4}$$

where W is the width of the trough. This will be made up of two components, that due to accumulation (a) and ablation (a negative) along the ice stream.

$$Q_a = \int_o^x W_a \, dx. \tag{5}$$

and that due to flow into the ice stream from flanking sluggish ice on the banks

$$Q_f = \int_o^x q_f \, dx. \tag{6}$$

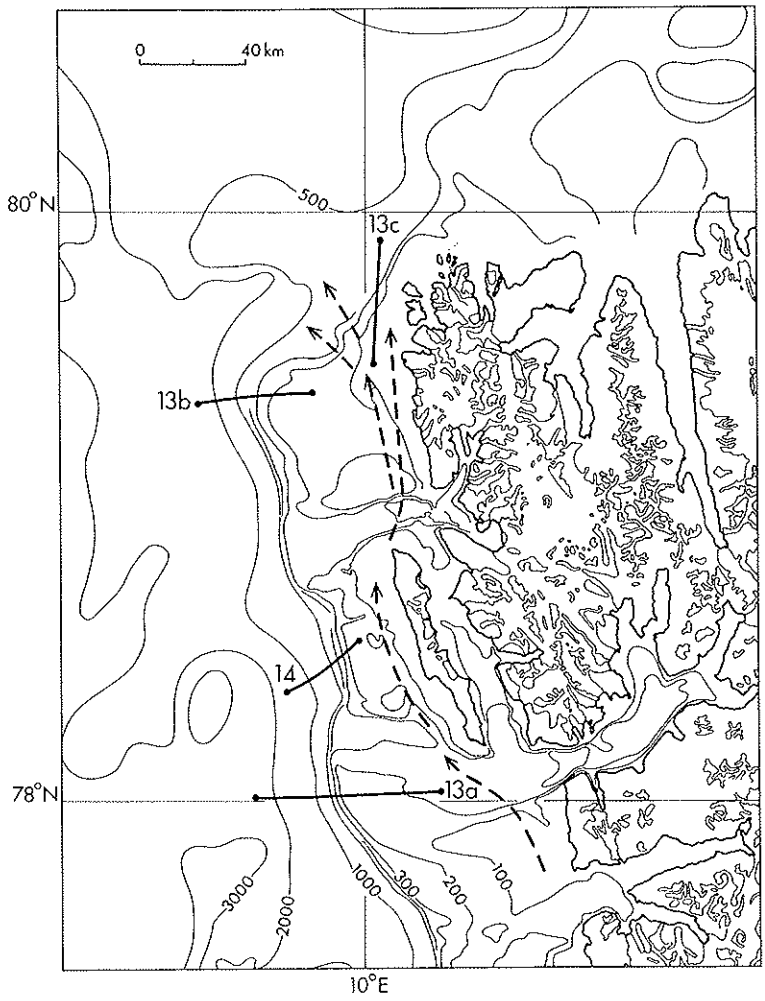

Fig. 11. Map of the west Spitsbergen continental margin showing Kongsfjorden (79°N) and Isfjorden (78°N), the glacially eroded troughs which emanate from them, and the intervening shallow banks. Large 'trough mouth fans' occur at the shelf edge. The predominant shelf currents flow north, starving the western shelf edge of sediment but feeding the shelf edge at 79.5°N to produce a zone of active progradation. Lines of sections shown in other figures are marked.

At any point, Q_s will be

$$Q_s = \int_o^x q_f \, dx + \int_o^x W_a \, dx. \qquad (7)$$

The slope across the margin of the ice stream (α_y) at any point will be

$$\sin^{-1}\alpha_y = \frac{(Q_s - Q_i)P_e^{\lambda}}{\rho g H_2^2}. \qquad (8)$$

Assuming the values of λ as calculated by Morland *et al.* (1984) and arbitrary and constant values of H_1, W and p_e, it is possible to reconstruct the confluent pattern of flow towards the ice stream and the distribution of basal velocity.

A simple expression is used to compute the resultant patterns of erosion and deposition (Boulton *et al.* 1984) which are determined by changes in the basal sediment transport rate, assumed to be proportional to U_b. Thus, the erosion rate ($\dot{E}$) is given by

$$\dot{E} = K_1 \frac{dU_b}{dx}. \qquad (9)$$

When this is negative, deposition occurs. I shall however assume that sediment transport occurs as a result of subglacial sediment deformation (Boulton & Hindmarsh 1987) and thus that

$$\dot{E} = K_2 \frac{d\tau_b}{dx}. \qquad (10)$$

To permit this, we expect very low values of effective pressure (p_e) because of the difficulties of drainage from the subglacial mass.

Figure 12a shows the flow paths and erosion deposition pattern for a glacier flowing over a surface containing a longitudinal trough where there is no significant calving. In a steady state, we would expect the zone of deposition near to the glacier margin to show thicker till units within the trough than on the flanking banks.

If the glacier flows into the sea, but the calving rate is small, inhibited perhaps by fixed sea ice, and if additional buoyancy in the terminal zone is enough to reduce P_e and thereby the basal shear stress, it will enhance the tendency towards subglacial deposition in the terminal zone (Fig. 12b).

If however the calving rate is very high, it may only be balanced by velocity in the high velocity zone where dU_b/dx and $d\tau_b/dx$ are positive, thus ensuring that erosion will occur as far as the glacier terminus (Fig. 12c). A further consequence will be to dump all the debris in transport immediately beyond the glacier terminus. Again we expect a strong contrast on the flanking banks where the glacier may terminate on land, with a marginal depositional zone, or in shallower water than in the trough which, because of a slower calving rate, will result in less erosion, or deposition on the banks.

If the ice stream begins to float on the shelf before the terminus, we would certainly expect a terminal depositional zone as p_e will go to zero at the grounding line (Fig. 12d). If it only floats at the shelf break, where p_e may decrease extremely rapidly, a terminal erosion zone may give way immediately to a proglacial dump (Fig. 12e).

Thus, in most circumstances we would expect a strong contrast between till thickness on the banks and in the trough.

(d) The shelf break and continental slope

No modern continental shelf break in a glacimarine environment lies in the proximal or ice-contact zone. To understand proximal and ice-contact shelf-break and continental slope processes we must refer to those localities where glaciers reached the shelf edge during glacial periods.

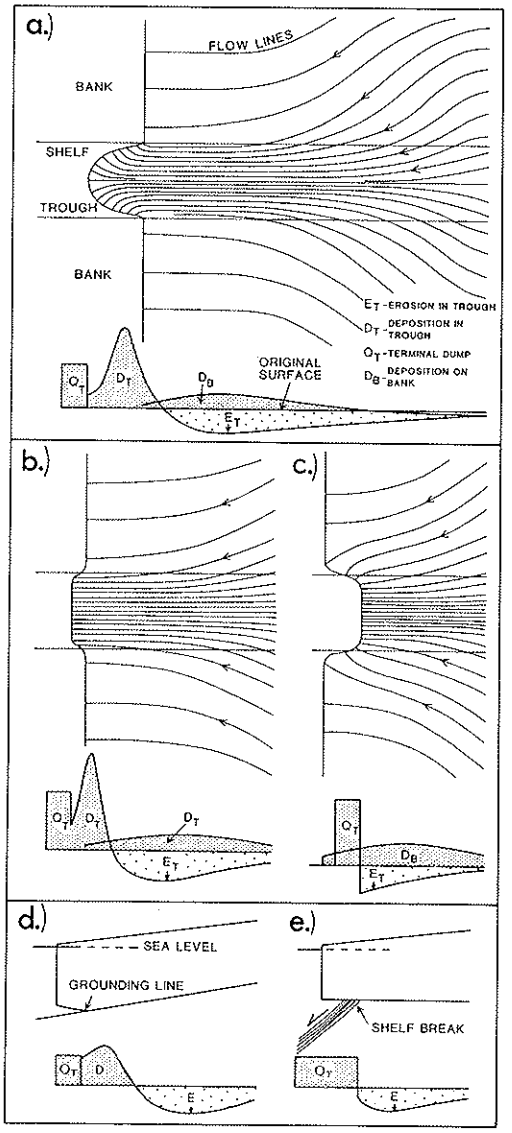

Fig. 12. Theoretical patterns of erosion and till deposition along shelf troughs and on the flanking banks. (a) Ice stream terminating on the shelf without significant calving. (b) Ice stream terminating on the shelf with some calving. (c) With very strong calving. (d) Shelf ice stream with floating terminus. (e) Ice stream floating at the shelf edge.

A major feature of the distal margins of glacially eroded troughs crossing many high-latitude shelves are '*trough-mouth fans*' where the degree of progradation of the shelf has been much greater than in the adjacent banks (Fig. 11). The sequence in such a trough mouth fan,

at the mouth Isfjordrenna, in west Spitsbergen, is shown in Fig. 13a. Coring reveals the uppermost unit to be a proximal glacimarine mud, capped by a gravelly lag. Where the mud has been completely removed by erosion, we find an underlying dense, massive and unfossiliferous diamicton, which is presumed to be till. It has been suggested in previous sections that thick glacimarine muds only develop in the proximal zone, which would imply that the mud unit reflects the advance of a glacier onto the outer continental shelf. If this is so, then it seems most likely that it forms part of a couplet with the underlying till, the latter reflecting glacier advance to the shelf edge, and the former the early stages of retreat. Below, beyond and above the till, strong reflectors indicate major progradation. This may reflect discharge of sediment from the tidewater or floating margin of a fast ice stream occupying the trough.

There is a contrast on the western Spitsbergen continental slope between the style of failure in front of trough-mouth fans and the intervening banks. In the latter, where till thicknesses are

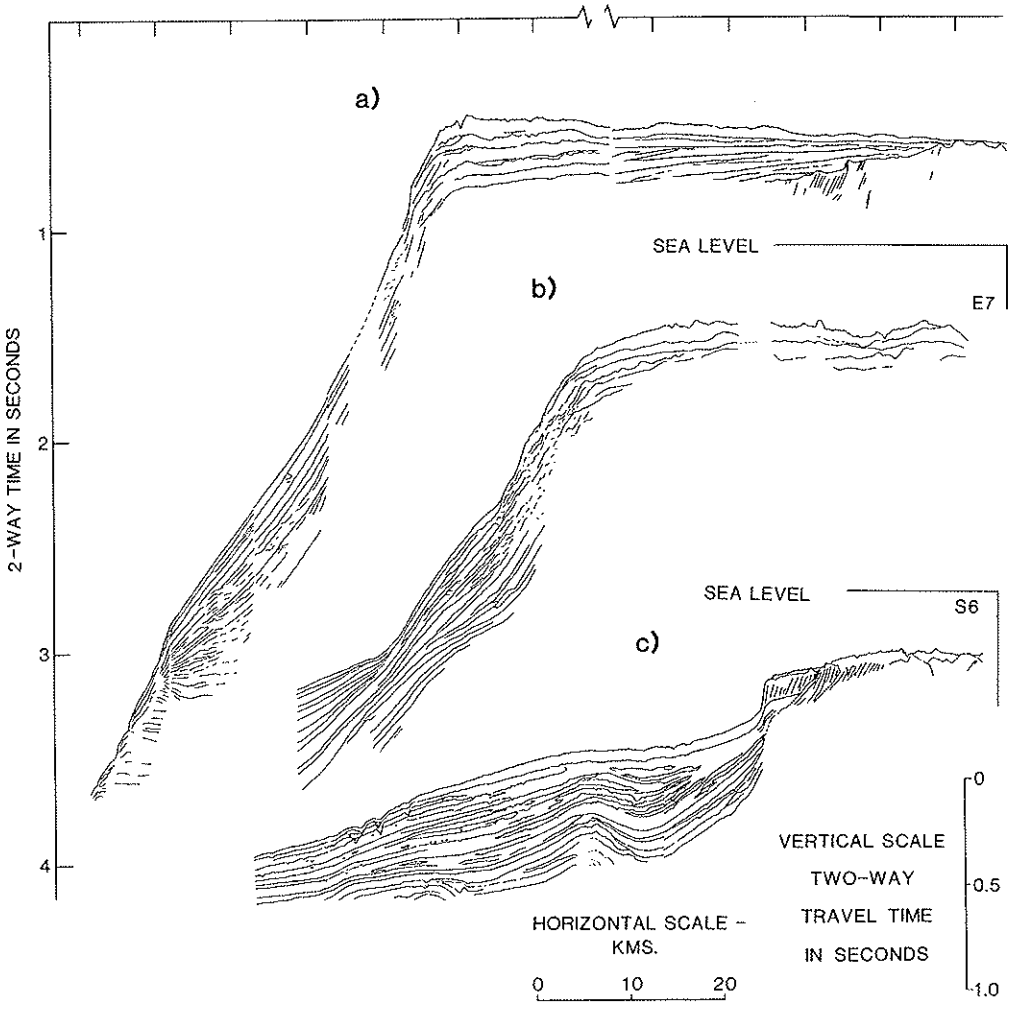

Fig. 13. Interpretation of air-gun records across the West Spitsbergen shelf edge. See Fig. 11 for location. (a) Section across the fan at the mouth of Isfjordrenna showing glacial couplets. (b) Thickening of sediment on the lower continental slope north of Kongsfjordrenna. A currently inactive margin where slumping of the upper slope feeds the lower slope. (c) Depositionally active north-western margin of the Spitsbergen shelf showing progradation on the upper slope and shelf break.

relatively large, deep-seated failure planes occur along which large sediment masses are displaced (Fig. 14). In the former, where till-tongues pass into acoustically layered sediments at the shelf edge no such large structures can be discerned, and it is presumed that mass-transfer occurs through numerous small scale failures and slumps.

It is clear from Fig 13a–b that current rates of sedimentation on the upper continental slope beyond trough-mouth fans are very low and that little sediment is discharged directly over the shelf-edge of western Spitsbergen. Geostrophic and tidal currents on the west coast of Spitsbergen produce a generally northerly drift of sea-floor sediment and surface water. This dominant long-shelf sediment drift is discharged into deep water across the northwestern shelf edge (Fig. 11), where, in contrast to the western shelf, evidence of active progradation is clearly seen on seismic profiles (Fig. 13c). This contrast between and 'active' northwestern shelf edge and continental slope and an 'inactive' western shelf edge and slope is reflected in the seismic stratigraphy. Whereas in the former the most recent seismic sedimentary units are involved in prograding, overstepping relationships on the upper slope and shelf (Fig. 13c), in the latter they show an on-lapping relationship lower on the slope (Fig. 13b). Indeed, in many profiles, this on-lapping of the lower slope can be seen to be the product of major slides and slumps on a continental slope of 3° to 6° (Fig. 14), and in some, successive major slumped units can be identified which are up to 140 m in thickness and 3–5 km in longitudinal extent.

It is suggested that advance of a glacier to the shelf edge disrupts the long-shelf sediment dispersal pathway, moves the proximal zone of surface-plume dominated sedimentation to the shelf edge, produces high rates of sediment discharge directly over the shelf edge and active shelf progradation (Fig. 13a). During periods when glaciers have retreated from the shelf, oceanic water penetrates onto the shelf and produces long-shelf sediment dispersion. High rates of primary sediment discharge over the shelf-edge cease, the glacially-oversteepened upper slope begins to fail and slumped masses accumulate low on the continental slope.

Part 2: The effect of glacial cycles and associated sea level changes on facies architecture

It is argued below that the facies architecture produced by a glacial cycle is the consequence of a temporal shift of the spatial distribution of facies described in part 1, in response to changing glacier position and changing glacially-controlled sea level. A model of glacially-controlled sea level is developed below, which is used to predict the distribution of principal facies elements in time and space through a glacial cycle. These theoretical distributions are then compared with evidence of glacially controlled sea level change and facies organization from Pleistocene and pre-Pleistocene sequences.

A model of sea-level change near to an ice sheet during a glacial cycle

The growth and decay of Pleistocene ice sheets has involved an exchange of mass of about 4×10^7 km^3 between the oceans (2.2×10^8 km^2 area) and ice sheets on northern Europe and North America (14×10^6 km^2 area – Antarctic and Greenland ice sheets underwent relatively little areal or volumetric change, at least during the last glacial cycle). This results in fluctuations of ocean level of about 120 m and changes in ice sheet thickness in mid-latitudes of up to 4 km. The cyclical concentration and dissipation of mass from mid-latitude ice sheets affects sea level in three principal ways: (i) in global eustatic changes as a direct result of ice volume change; (ii) in local isostatic crustal flexure in response to cyclical loading and unloading of the crust by ice and water; (iii) local changes in the sea surface level in response to the gravitational attraction of changing masses.

These components of sea level will have an effect on *relative sea level* (R_s), which is the local level of the sea in relation to a fixed point on the solid earth surface. Using an up-positive, down-negative convention:

$$R_s = E_s + I_s + G_s$$

where E_s, I_s and G_s are the net changes in eustatic sea level, in isostatic displacement of the crust and gravitational change in sea level surface respectively in relation to an assumed interglacial equilibrium condition. These variables are treated independently for simplicity's sake.

For the purpose of illustration a two-dimensional ice sheet model is used (Boulton *et al.* 1984) in which expansion and decay of an ice sheet is approximated by a sequence of steady states which are determined by snow-line elevations. This is used in preference to a time-dependent ice sheet model (Hindmarsh *et al.* 1987) merely because it is easier to match a

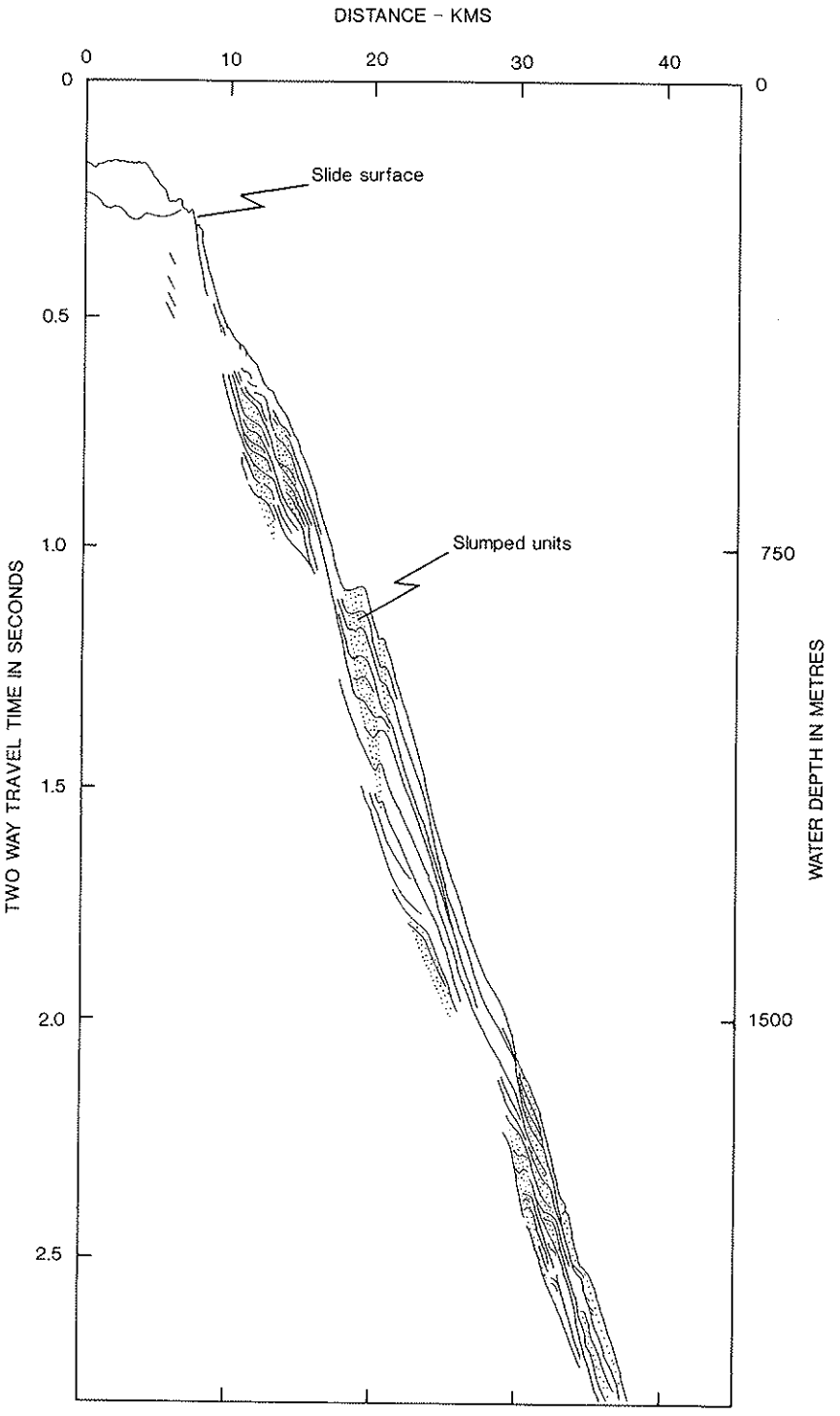

Fig. 14. Interpretation of an air-gun record showing major slumps on the upper continental slope of west-Spitsbergen. Slumps comprise two major elements, a smooth slide surface below which lies a longitudinally-compressed mass which has moved along the slide plane and accumulated at its foot. They show a typical sigmoidal reflector patterns. See Fig. 11 for locations.

prescribed pattern of glacier variation in time and space.

In computing isostatic deflection, we assume the response of the solid earth to ice sheet loading to be governed by a rigid, elastic lithosphere and an underlying viscous asthenosphere. The stiffness of the lithosphere will ensure that gravitational equilibrium, if and when achieved, will be a regional equilibrium, rather than a local one beneath every loaded point. As a consequence, downward deflection will occur both beneath and slightly beyond the loaded area, and an upward bulge will occur beyond that. The pattern of depression and uplift will be determined by lithosphere elasticity, whilst the rate of response will be determined by flow in the asthenosphere. Following Turcotte & Schubert (1982), the deflection [$W_{(x)}$ – positive downwards] beneath a point load (V_i) will be:

$$W_{(x)} = \frac{1}{8D} V_i \alpha^3 e^{-x} (\cos x + \sin x) \quad (11)$$

where D is the flexural rigidity of the lithosphere, $x = \frac{|x|}{\alpha}$ and $\alpha = \left(\frac{4D}{\rho m g}\right)^{1/4}$

and ρm is the density of the asthenosphere. Flexure is computed by assuming the ice sheet load to consist of a series of point loads.

The rate of change of elevation of the surface of the lithosphere is calculated following Oerlemans & van der Veen (1984), and is given by

$$\frac{\delta h_b}{\delta t} = D_a \frac{\delta^2}{\delta x^2} (h_{b0} - h_b + W) \quad (12)$$

where h_{b0} is the initial elevation, D_a is the diffusitivity of the asthenosphere and is given by $D_a = gH^3/3\nu$ where H^3 is the thickness of the asthenosphere and ν its viscosity. H and ν are not known, but Walcott (1973) has estimated values of D_a from North America and Scandinavia. Values of $D_a = 1.67$ m^2 s^{-1} and $D = 5 \times 10^{23}$ Nm were used.

Figure 15 shows progressive deflection of the crust in response to prescribed glacier growth and decay using the above scheme. Deflection does not achieve equilibrium with ice load during glacier expansion, and as a result, maximum crustal depression occurs during deglaciation. A proglacial bulge occurs which is progressively displaced as a wave beyond the advancing front

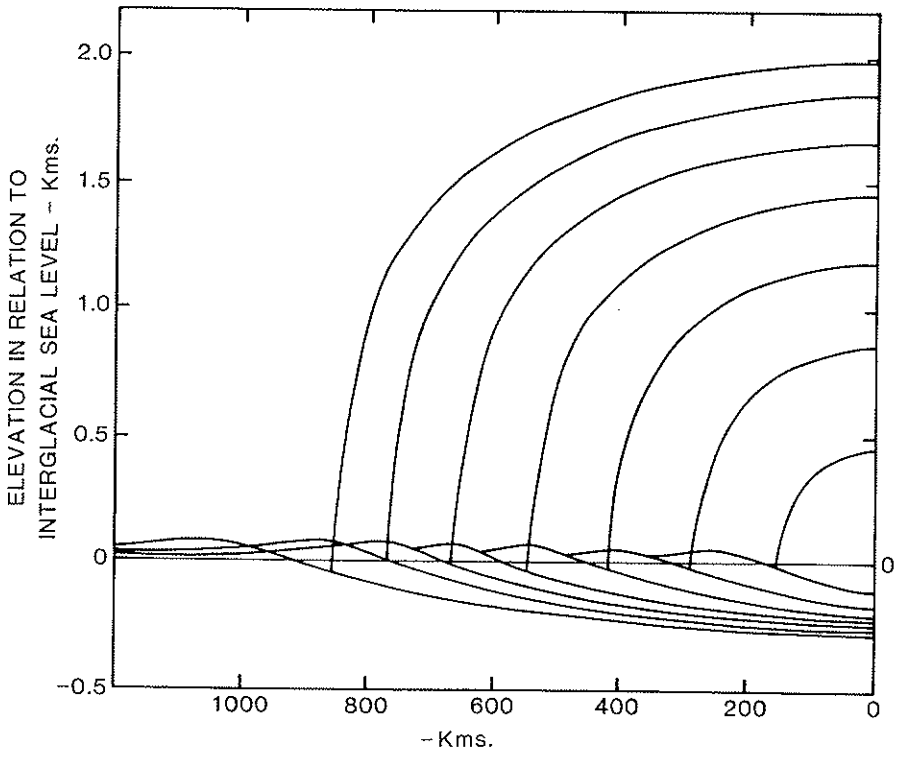

Fig. 15. Progressive crustal deflection produced by glacier growth.

of the ice sheet.

The gravitational attraction of the ice sheet mass for the water surface was calculated using the analysis of Peltier *et al.* (1978).

The pattern of relative sea level change near to an ice sheet in response to the ice sheet's expansion and decay was computed for an ice sheet cycle in phase with the global eustatic sea level cycle (Fig. 16a), and for cycles which both lead (Fig. 16c) and lag (Fig. 16b) the global eustatic cycle by 4.25 ka. The first reflects the pattern expected around the ice sheet which exhibits the largest volumetric change and thus dominates the global eustatic cycle (e.g. the Wisconsinan Laurentide ice sheet) or a smaller one in phase with it (e.g. the European Weichselian ice sheet during decay); the second is a smaller ice sheet which leads the dominant ice sheet's fluctuations (e.g. the Devensian British ice sheet during its decay phase); and the third one which lags the dominant ice sheet (e.g. the Weichselian West Spitsbergen ice sheet in its decay phase).

The relative sea level changes which would occur at a series of points at different distances from the point of ice sheet nucleation for each of these cases are shown in Figure 17. They all share similar features.

(i) In the area far beyond the maximum extent of the glacier, a symmetrical cycle of relative sea level change is presumed to have a similar phase and amplitude to the global eustatic cycle (Fig. 17−1). Nearer to the ice sheet, in the zone of the extra-marginal bulge (Fig. 17−2), the amplitude is significantly greater than that of the global eustatic cycle, whilst there is a sea level phase lead where local ice sheet growth and decay leads the global eustatic cycle.

(ii) In areas overriden by the glacier relative sea level change is asymetric, with the maximum sea level regression preceding glacier advance over any site, and the maximum transgression following retreat (Fig. 17, 3−5).

(iii) In Fig. 16 the rates of advance and decay of the northern margin of the ice sheet are prescribed to be less than those of the southern margin. As a consequence, the ice sheet residence time at any point a given distance inside the northern margin will be greater than at a similar distance from the southern margin. The isostatic effect will therefore be greater in the north, and deglaciation will tend to coincide with phases of much higher sea level (Fig. 17−5) than at the southern margin, where phases of relatively low sea level will be succeeded by phases of transgression (Fig. 17−3).

(iv) Because of the wide range of rates of glacio-isostatic uplift during deglaciation between the maximum extent of ice and the centre of glaciation, there will, at some point, be a sustained equivalence between rates of eustatic sea level rise and crustal uplift, leading to a static relative sea level (Figs 17−3b, 17−5a-c).

There are several elements of dissimilarity.

(i) The extent of the zone in which isostasy dominates relative sea level is greatest where the local glacial cycle lags the global eustatic cycle and least when the local cycle leads the global eustatic cycle;

(ii) Where the local ice sheet lags or is in phase with the global eustatic cycle, there is a relatively simple contrast between the eustatically-dominated zone of deglacial sea-level transgression (Fig. 17−1, 2) and the isostatically dominated zone of deglacial sea-level regression (Figs 17−4, 17−5ab). However where local deglaciation leads global eustasy the early decay of the isostatic component before significant eustatic rise, produces a pattern of sea level regression followed by transgression in a broad zone near to the ice sheet's maximum extent (Figs 17−3, 17−5c).

Figure 18 shows the isobases produced as a consequence of the glacial cycles shown in Fig. 16a. These represent the current disposition of planes which lay at sea level at the times given on the diagram. Their form reflects the net result of the isostatic warping of the crust and the eustatic sea level change which has occurred since those times. They are natural bounding surfaces for marine sediment packages. They show how beach sediments of a given age which formed during the glacial cycle will tend to lie above modern sea level in the isostatically-dominated zones, and how their lateral equivalents will lie well below sea level in the eustatically dominated zone. Important characteristics are as follows.

(i) The marine limit in the isostatic zone is diachronous and dips at a smaller angle than isobases. Only instantaneous ice sheet disappearance will give an isochronous marine limit.

(ii) The location of the extra-glacial isostatic 'bulge' is indicated by a depression of isobases in the eustatic zone.

(iii) They show evidence of a regression followed by transgression during glacier build up in the area within and just beyond that occupied by the glacier at its maximum extent.

(iv) They show that in the case of a glacier whose decay leads the global eustatic decay, regression followed by transgression during deglaciation occurs in a zone near to the maximum extent of the glacier.

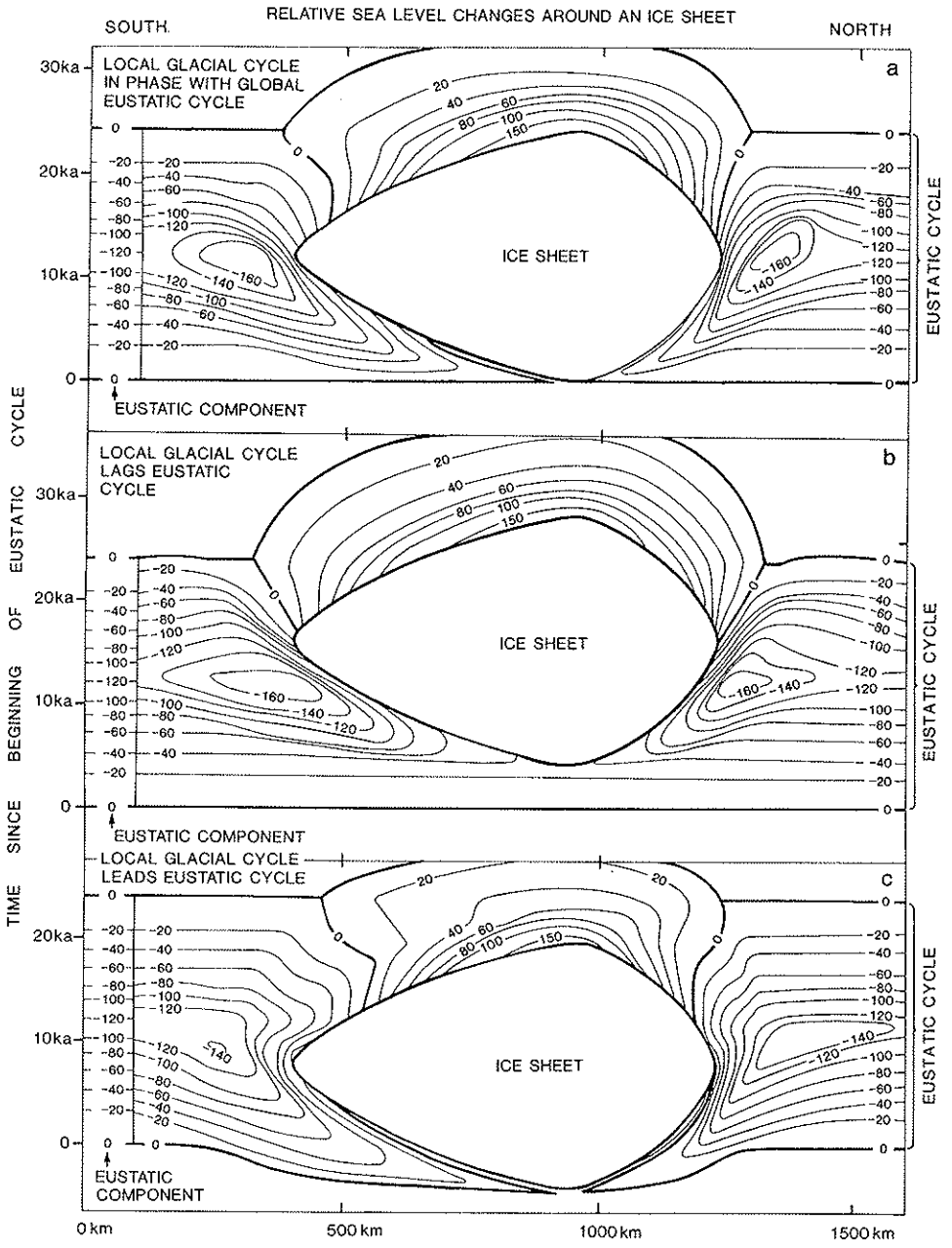

Fig. 16. Patterns of relative sea level change in space and time produced by expansion and decay of an ice sheet resulting from interaction of eustatic, isostatic and gravitational components of sea level change. (a) Local ice sheet cycle in phase with dominant global eustatic cycle. (b) Local cycle lags global cycle. (c) Local cycle leads global cycle. The component of sea level change due to the global eustatic cycle is shown on the left of the diagrams. Elapsed time is shown from the beginning of the global eustatic cycle.

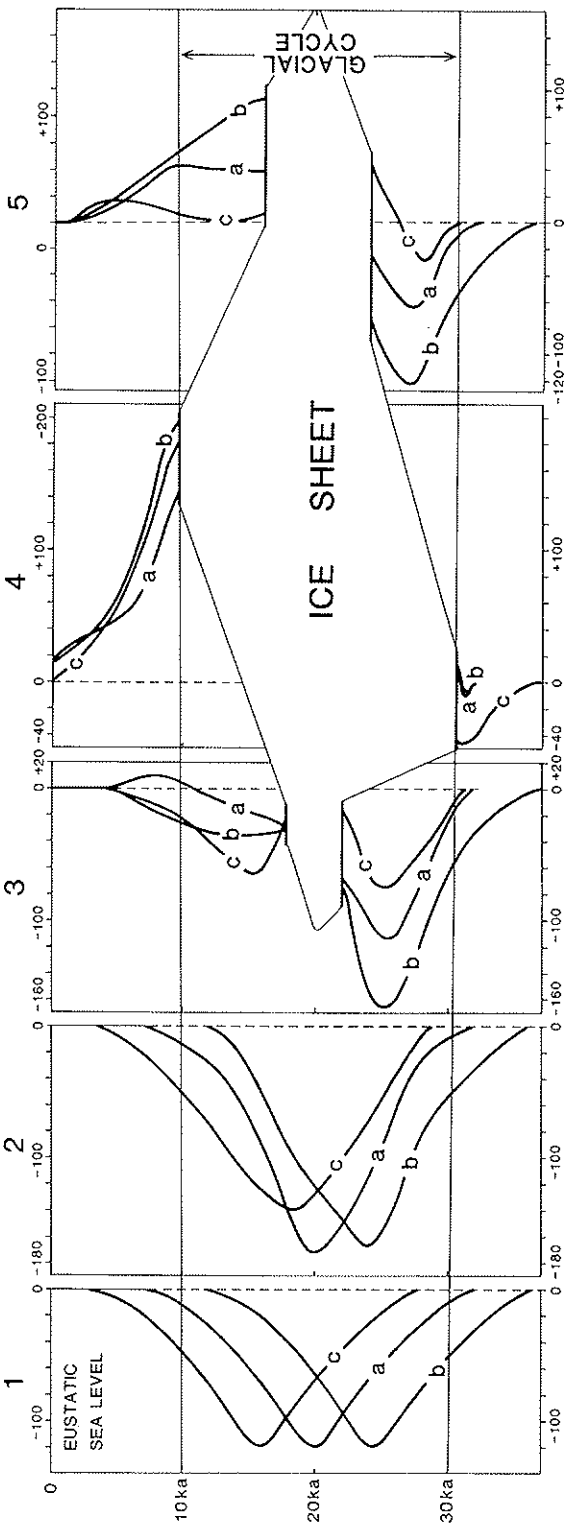

Fig. 17. Relative sea level change through a glacial cycle at localities 1–5 which occur at distances of 1 = 0 km; 2 = 275 km; 3 = 440 km; 4 = 800 km and 5 = 1190 km in Fig. 16. Curves marked *a*. are those where the local glacial cycle and global eustatic cycle are in phase, those marked *b*. where local cycle lags the global cycle, and those marked *c*. where the local cycle leads the global cycle. The glacial cycle occurs between 30 and 10 ka. Leads and lags can be seen from its relation to the eustatic cycles shown at locality 1.

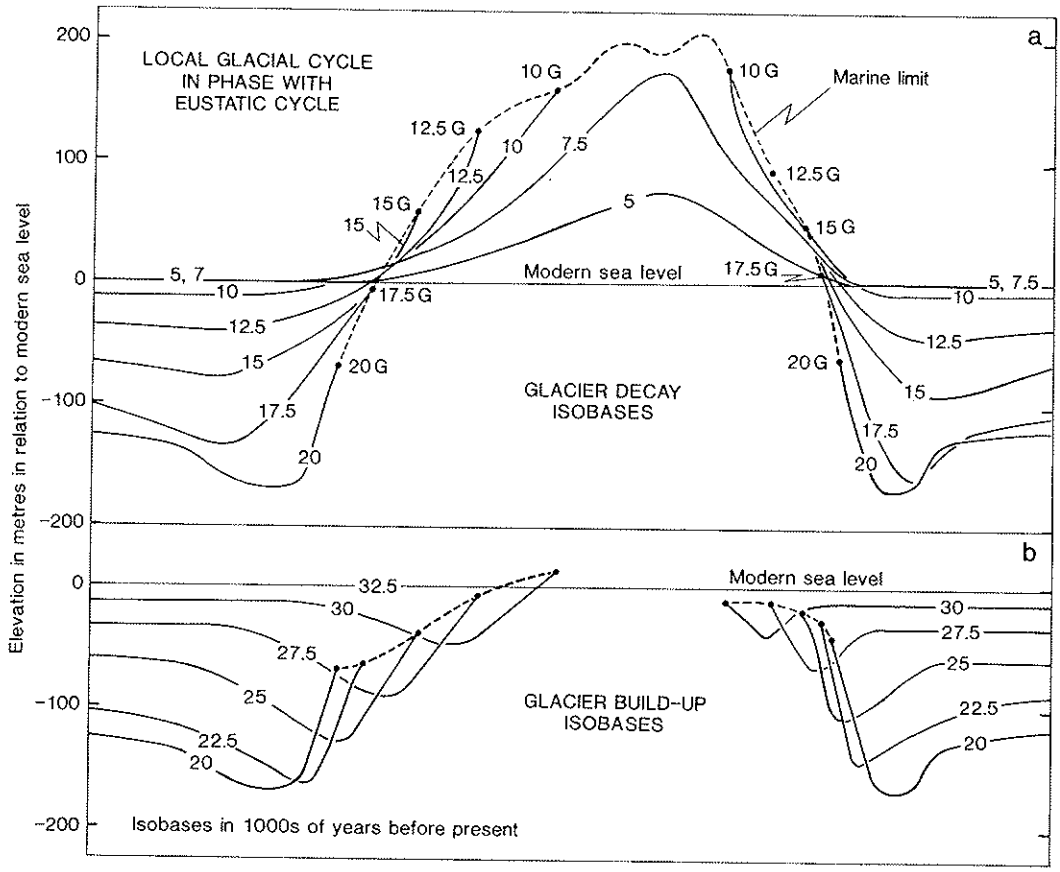

Fig. 18. Two dimensional form of isobases dating both from the period of ice sheet expansion and the phase of ice sheet decay from the model in Fig. 16 where the local glacial cycle is in phase with the global cycle. Isobases show the current form of surfaces which lay at sea level at the stated time.

Glacimarine facies architecture on the land margin and shelf: theory

The simple spatial model of glacimarine facies developed in part 1 relates the character and rate of accumulation of sediment at any site to its distance from the glacier, the slope of the substratum and its relation to sea level. If this is combined with a model of glacier extent and sea level change, such as that in Fig. 16, the distribution of sedimentary environments in space and time can be reconstructed. An example is shown in Fig. 19 for a local glacial cycle in phase with the global eustatic cycle.

Figure 20 illustrates the sedimentary sequences which would develop in response to this temporal and spatial shift of environments. Figure 20a shows the vertical sequences which would develop at given distances from the centre of glaciation at all elevations, and Fig. 20b the horizontal sequences at specific elevations. It combines the sedimentation rate model from Fig. 6 and a model of the shoreline processes in Figs 5 and 22 with the sea level/environment models in Figs 17 & 19. Uplifted marine sequences in the isostatically-dominated zone are shown by 4–10 in Fig. 20a and largely coincide with the glaciated area, apart from sequence 10 at the northern margin of the ice sheet, where longer glacier occupancy has produced stronger crustal deflection reflected in a transgression beyond the limit of glaciation. The flanking eustatically-dominated zones suffered low glacial sea levels. The transgression limit (= marine limit) and regression limit are as shown in Fig. 16. Several other attributes are worthy of note.

(i) Glacimarine muds only survive above sea level in the areas of greatest uplift and well below the marine limit.

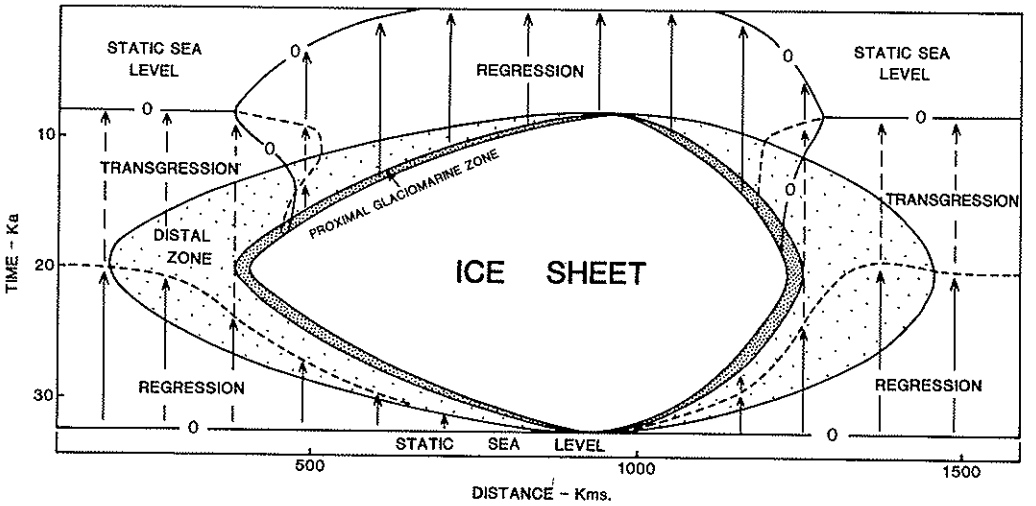

Fig. 19. Distribution of environments in space and time during a glacial cycle in which the local ice sheet is in phase with the global eustatic cycle (c.f. Fig. 16a).

(ii) No normal marine muds survive above sea level.

(iii) The regression limit pre-dates the glacial maximum and is diachronous in the isostatic zone although it is synchronous with the glacial maximum in the eustatic zone (Fig. 18). Early glacial marine sediments thus survive at a high elevation in the isostatic zone, where the regression limit is high and where it is not removed by glacier erosion (Fig. 20–9), and only at low elevations in the eustatic zone, where erosion beneath the low regression limit removes them (Figs 20–1, 2, 10, 12).

(iv) It has been argued (Boulton 1982) that the peripheral zone of an ice sheet is a zone of deposition and the internal zone one of erosion. Early glacial (and pre-glacial) sequences near to the maximum extent of the ice sheet will tend to be preserved and capped by till (Fig. 20–9) whilst those nearer the interior of the ice sheet at its maximum (Figs 20–6, 8) will tend to be removed by subglacial erosion.

(v) Major erosional notches along the shoreline are presumed to reflect long periods of stable sea level. They occur in the eustatic zone where eustatic change ceases long before the isostatic component has decayed, and in the isostatic zone where rates of isostatic uplift and eustatic sea level rise are similar. This often occurs near the marine limit (Fig. 17–5a), and may also lead to major sediment aggradations at sea level due to the high rates of sediment supply in the glacimarine environment (Fig. 20–9).

Figure 20b shows expected sequences at specific elevations above and below sea level. It utilizes an erosional/depositional theory (Boulton 1982) which predicts net erosion in the inner zone occupied by an ice sheet, net deposition in an outer zone, and deposition without erosion in an outermost zone, which is the only area where immediately pre-glacial sediments will be preserved. In deep water (−200 m) we expect a complete late-glacial and post-glacial record to be preserved. In shallow water (−60 m), we expect evidence of early glacial sea-level regression to be preserved in the outer glacial zone, but strong marine erosion of the glacial, late-glacial and post-glacial sequence. Above at increasing heights above interglacial sea level (+100 m, +150 m) we expect the lateral extent of uplifted glacimarine sediments to become progressively more restricted.

Figure 22 shows the altitudinal distribution of the major sediment facies groups resulting from a glacial cycle. The upper limit of beach and littoral facies is marked by the marine limit. Its lower limit is presumed to lie some 10 m or so below the regression limit. It is assumed that in unsheltered environments, glacimarine mud will not accumulate in less than 30 m of water (Boulton *et al.* 1982) and that its deposition will cease as glaciers withdraw from the catchment. In the isostatic zone the topographically highest glacimarine mud units will be the oldest muds and lie about 30 m below the marine limit. In the eustatic zone of deglacial marine transgres-

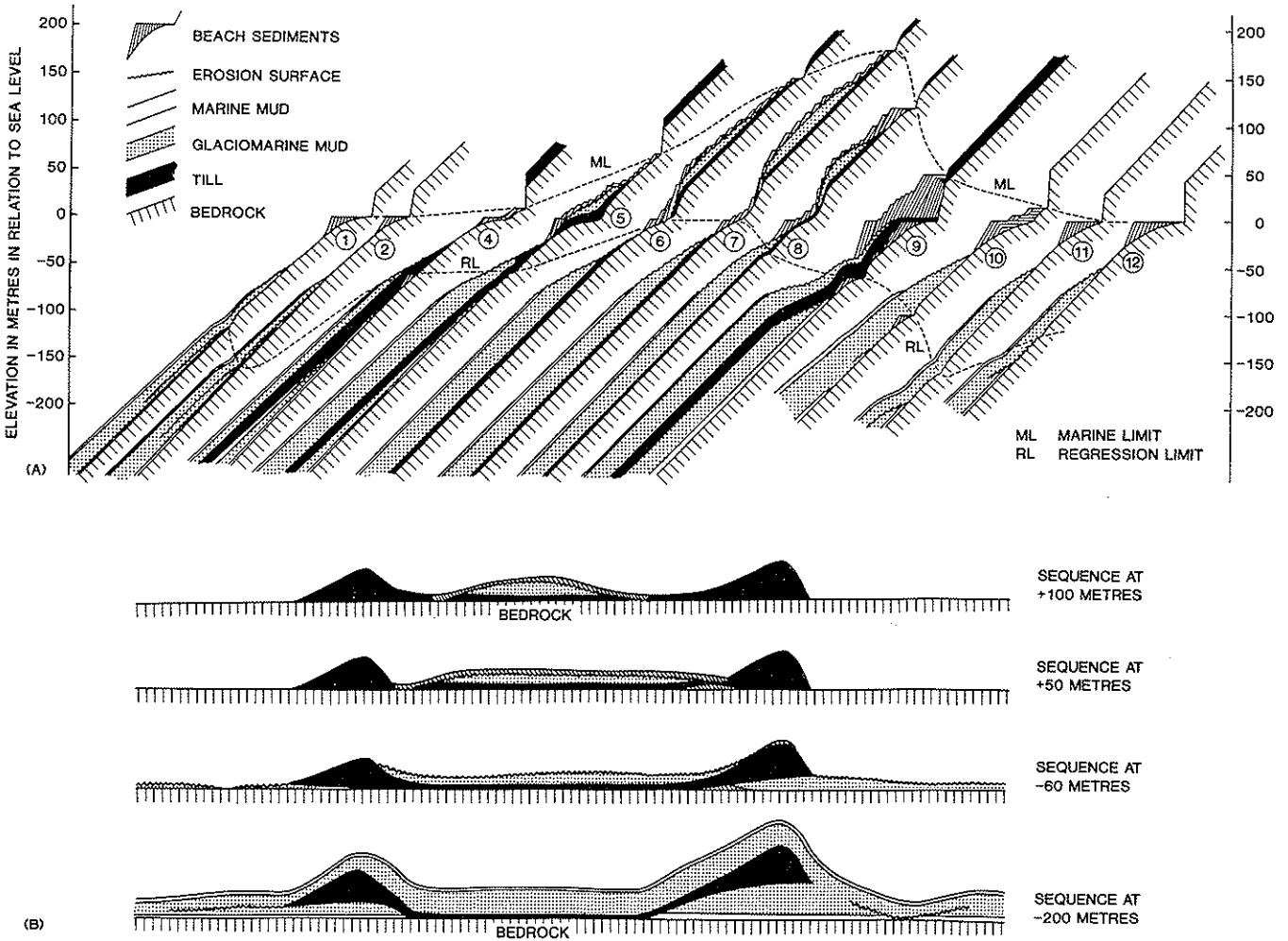

Fig. 20. Facies distribution produced by a complete glacial cycle in which the local cycle lags the global cycle (c.f. Fig. 17). (a) Onshore/offshore sections at specific distances to the north and south of the centre of glaciation. (b) Longitudinal sections at specific elevations above and below sea level.

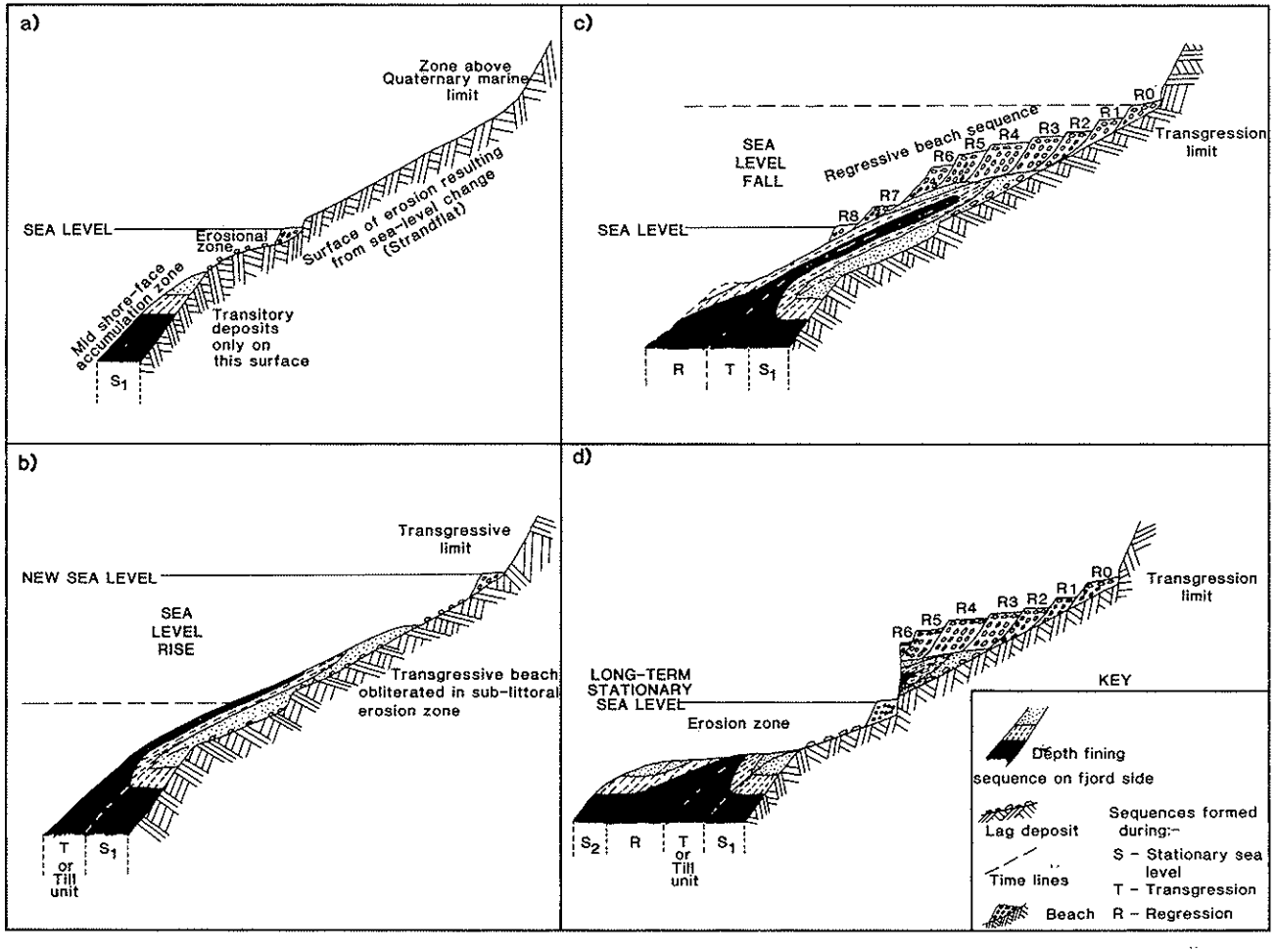

Fig. 21. Sedimentary sequence in the nearshore zone resulting from a glacial-isostatically dominated sea level cycle in a site just beyond a glacial maximum in an area where the local cycle lags the global cycle. (a) Facies distribution during interglacial. (b) Consequence of sea level rise resulting from dominant glacio-isostatic crustal depression. The transgressive unit (T) could represent a till if the site had been overridden by a glacier. (c) Late-glacial sea level regression. (d) Erosional notch produced during static interglacial sea level.

sion the topographically highest glacimarine muds will be the youngest muds, whose deposition will cease as glaciers withdraw from the catchment area. The youngest glacimarine muds at any elevation can be determined for Fig. 22 by superimposing this on the isobase plot in Fig. 18.

In the interglacial North Sea muds only accumulate in water depths greater than about 70 m. Similar upper limits for mud deposition occur on other temperate continental shelves. In the isostatic zone, the maximum elevation of interglacial muds will depend upon the net uplift which has occurred since glacier withdrawal from the catchment. In the eustatic zone, the highest interglacial muds will be youngest and lie at about 70 m below modern sea level.

The location of sea level is particularly important, for a small change in water depth in the nearshore zone can lead to rapid changes of sedimentary environment from one of mud deposition to one of strong erosion and beach sediment accumulation. The zone above and below interglacial sea level, which is swept successively by these regimes as sea levels rise and fall during glacial cycles, is one of considerable sedimentary complexity. The character of the sequences produced by a simple cycle of sea level rise and fall and consequent displacement of shore-face facies zonation in an isostatically-dominated zone is shown in Fig. 21a-d. The transgressive beach tends to be obliterated by the succeeding erosional phase, except at the transgression limit, whilst other components of the transgressive sequence tend to be removed in the erosional zone during sea level fall. Thus, only at lower elevations, where there has been a longer period of sedimentation and shorter erosional phases, are muddy sediments preserved beneath beach sediments. The sequences preserved above interglacial sea levels, which in the Quaternary are the most directly accessible, tend to reflect very short timespans during late-glacial sea level regression. Complete sequences will tend to lie in deep water.

Glacimarine facies architecture on the land margin and shelf: examples

The dominant control on global eustatic sea change during the last glacial cycle has been the fluctuation of mass of the Laurentide ice sheet. Examples of local relative sea level history and glacimarine facies architecture have been chosen from the areas of the last European ice sheet whose decay has been roughly in phase with the Laurentide, from the west Spitsbergen ice sheet margin which lagged the Laurentide and the British ice sheet which led it.

a. Patterns of relative sea level change. Figure 23 shows patterns of relative sea level change and Fig. 24 the form of isobases along radial transects across the areas of Europe, Spitsbergen and Britain occupied by ice sheets during the Late Weichselian.

Deglaciation of western Spitsbergen clearly lagged the decay of the Laurentide ice sheet (Boulton *et al.* 1982; Mangerud *et al.* 1987). As a consequence, it produced the most extensive zone of isostatically-dominated late-glacial and post-glacial sea level change as a proportion of ice sheet radius of the three ice sheets used here as examples. This effect is smaller in the case of the European ice sheet and least in the case of the British ice sheet, as we would expect from the phasing of deglaciation in relation to that of the Laurentide ice sheet (cf. Fig. 16). Major

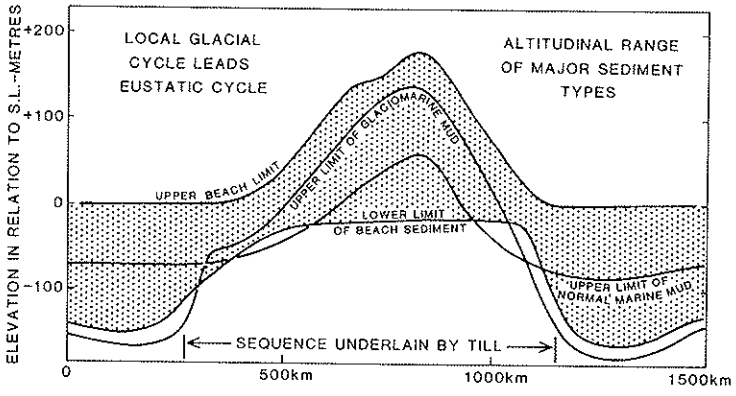

Fig. 22. Altitudinal range of major marine sediments types produced during a complete glacial cycle.

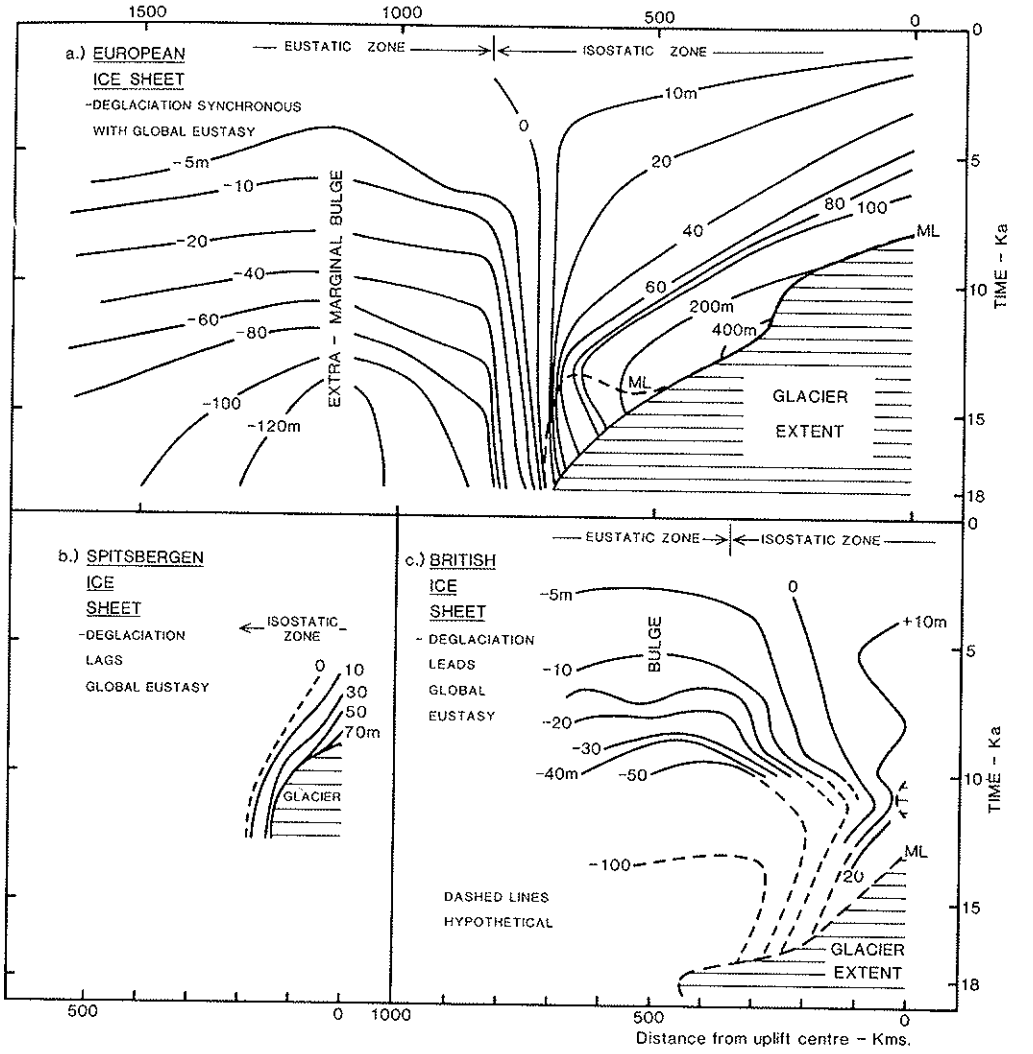

Fig. 23. Relative sea level change in time and space inferred from direct geological evidence. (a) Along a radial transect across the Weichselian area of the European ice sheet, through the western Baltic and eastern North Sea. (b) Along a radial transect across the area occupied by the Late Weichselian West Spitsbergen ice sheet (see Fig. 25 for location). (c) Along east coast of Britain across the area occupied by the Late Weichselian ice sheet.

global deglacial sea level rise begins at about 14 ka (Mix & Ruddiman 1985), whilst major European deglaciation begins at about 15 and 13 ka (Boulton *et al.* 1985; Lundqvist 1986), major deglaciation of parts of the British ice sheet had already occurred by 15 ka (Coope & Brophy 1972) and major West Spitsbergen deglaciation took place after 11–10 ka (Boulton *et al.* 1982; Mangerud *et al.* 1987).

In the case of Britain there is also evidence of a major late glacial sea level regression followed by transgression which the model (Fig. 16) predicts should occur where local deglaciation leads the global eustatic rise, due to an early decay of the glacio-isostatic component of relative sea level before a major eustatic sea level rise. In the Irish Sea basin, McCabe & Eyles (1988) and McCabe *et al.* (1986) have argued for sea levels up to 100 m above sea level at the time of deglaciation, whereas Holocene sea levels on the margin of the basin show a major transgression from −20m at 9 ka to modern sea

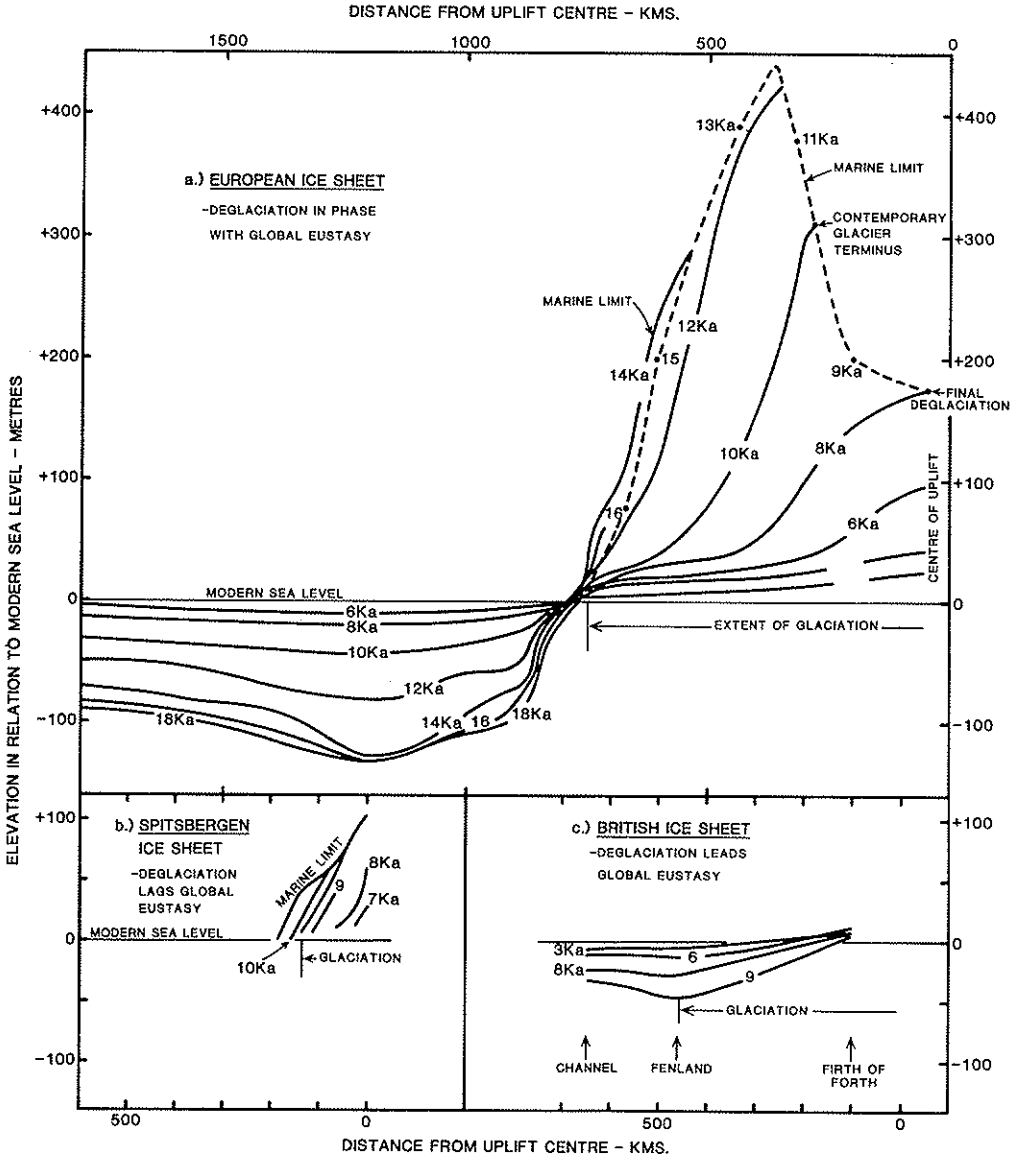

Fig. 24. Isobases along the same transect lines shown in Fig. 23.

level by 2 ka (Tooley 1978). A similar pattern can be inferred on the eastern coast of Britain (see next section) although the late glacial marine limit was significantly lower than at similar latitudes on the west coast.

The patterns of isobases for Europe and Britain (Fig. 24) also show a trough in the proximal part of the eustatic zone which probably reflects collapse of an extra-marginal bulge.

b. Patterns of facies distribution. Glacimarine facies architecture in an area where local deglaciation lagged the dominant eustatic cycle is well demonstrated in Spitsbergen. Figure 25 shows a map of the elevation of the marine limit over the Spitsbergen archipelago. It appears to reflect isostatic uplift in response to decay of two major Late Weichselian ice domes, one over the eastern part of the main islands

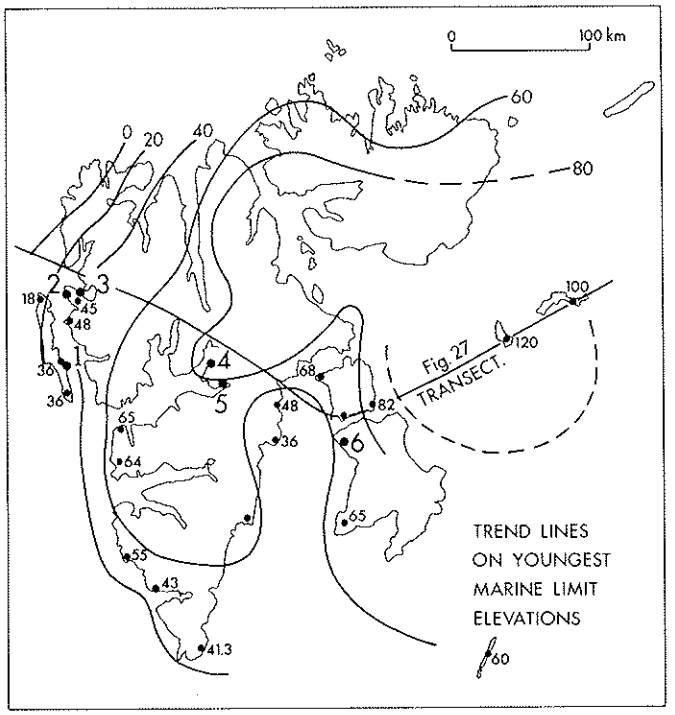

Fig. 25. Map of Spitsbergen showing the location of sites shown in Fig. 28 and the transect in Fig. 27.

of Vestspitsbergen and Nordaustlandet and another to the east of the archipelago. Fig. 26 shows a transect across these domes onto which isobases have been projected along lines parallel to the marine limit from sites near to the line of transect. If we assume that the highest relative sea level at any site is contemporary with deglaciation at that site, the intersection of isobases with the marine limit gives the age of deglaciation (c.f. Fig. 18). Thus, on the western side of the Spitsbergen ice dome, deglaciation of the west coast commenced prior to 10 ka and the ice dome in the vicinity of Kong Karls Land disappeared at about 10 ka. The marine limit is diachronous within the area covered by the ice sheet but isochronous in the area on the west of Spitsbergen not covered by the ice sheet.

A series of sections near to the transect show coarsening-upward sequences reflecting lowering of relative sea level. The highest elevations at which glacimarine muds have been found preserved generally lie between 20 and 30 m below the marine limit, which is similar to the depth below which muddy sediments tend to accumulate in exposed locations in modern fjords. Figure 27 shows sedimentary logs at several sites across the transect shown in Fig. 26. For the central area, where the marine limit is high above modern sea level, there is an upward sequence of till, followed by muddy glacimarine sediment of a variety of facies, overlain uncomfortably by coarse littoral sediments deposited during isostatically-dominated sea level fall (sites 3–6, fig. 27). At the limit of late Weichselian glaciation on the west coast of Spitsbergen, isostatic depression of the crust was still sufficiently strong to produce a high marine limit and permit mud to accumulate at some sea level sites. The lowest mud units are presumably contemporary with or may even pre-date the maximum of glaciation. Further west, the Late Weichselian marine limit is so low to have precluded deep-water mud accumulation above modern sea level, and coarse littoral deposits of the Late Weichselian/Holocene sea level regression lie directly above similar deposits of a regression from an earlier high sea level associated with a major glacial phase (sites 1–2, fig. 28). Further west still, the marine limit is presumed to fall below modern sea-level.

Sedimentary sequences produced by complete glacial cycles in sheltered fjords, well below the depth likely to be influenced by sea

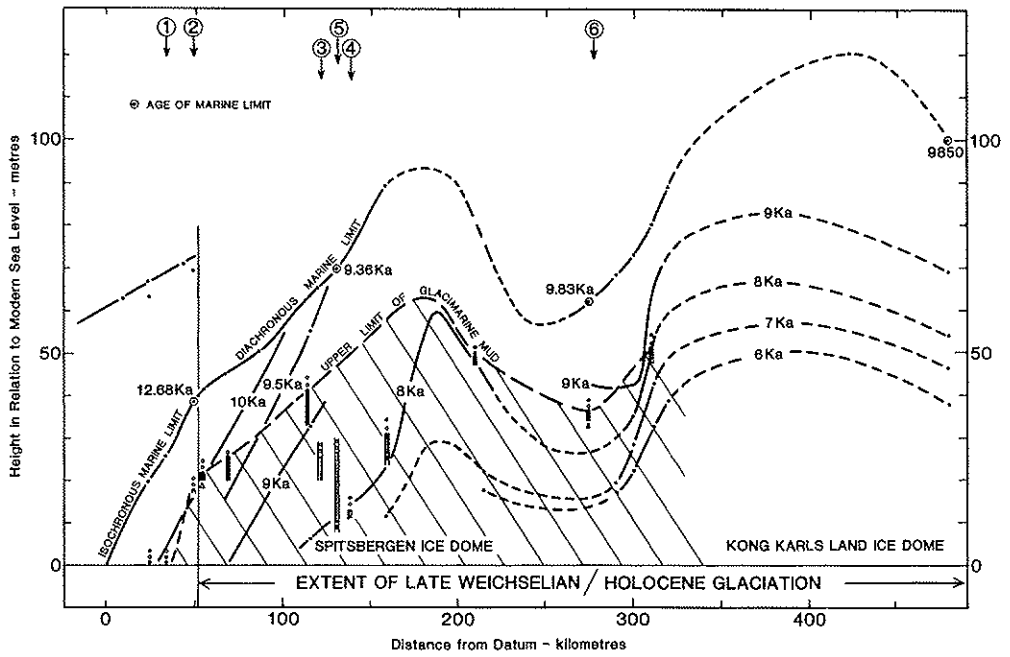

Fig. 26. Section across Spitsbergen showing the elevation of the Late Weichselian marine limit and isobases (in the west). The upper limit of glacimarine mud is shown and the location of important sections (triangles show till, vertical lines show glacimarine mud, and circles show beach sediment). Beyond the extent of Late Weichselian glaciation, an earlier, probably Early Weichselian marine limit survives, relating to uplift after glacier expansion to the shelf edge. The age of the marine limit, which is presumed to approximately date deglaciation, is based at 50 km on Mangerud *et al.*, (1987), at 140 km and 280 on Boulton *et al.*, (1982) and at 490 km on Salvigsen (1981). 1–6 show the locations of sections illustrated in Fig. 27.

level change (e.g. Fig. 20b: −200 m), have not, to my knowledge, been cored through in areas of modern glaciation. We do not expect them to undergo the same strong deep water scouring as sequences on open shelves, and if we assume that sea level change has a minor influence on sedimentation, only glacier proximity and sea bottom form will influence sedimentary sequences.

It was argued in part 1 that extensive glacimarine mud sedimentation only occurs on the middle and outer shelf when glaciers expand onto the shelf, bringing it within the zone of heavy fall-out from turbid plumes and displacing energetic ocean waters. When this occurs, we expect a full glacial cycle to show an upward sequence of till (partly made up of remoulded glacimarine sediment produced during the advance) and mud-dominated glacimarine sediment with evidence of current scour and reworking of the surface produced after deglaciation (Fig. 30). The failure of the Late Weichselian Spitsbergen ice sheet to expand over Spitsbergen's western shelf explains why there does not appear to be an extensive Late Weichselian glacimarine mud blanket on the outer shelf.

Glacimarine muds below the depth of modern wave induced scour on the West Spitsbergen Shelf, the Barents Shelf, the southern Iceland Shelf, in the North Sea, and many other high latitude shelves (Elverhøi *et al.*, 1983; Boulton *et al.*, 1988) tend to have armoured surfaces with predominantly reworked sands and muds in pockets on their surfaces. This may partly reflect low early Holocene sea levels, but the persistence of scour to the present day suggests that the extension of energetic oceanic waters onto interglacial shelves is a major cause. It is very likely that many glacial and glacimarine diamicton surfaces become armoured due to scour in late-glacial or early interglacial times, and thus that the major part of the glacial and glacimarine sediments removed from shelves in interglacials are removed at an early stage.

A quite different facies architecture to that in Spitsbergen is found in Southern Britain where deglaciation led global eustasy. On the eastern

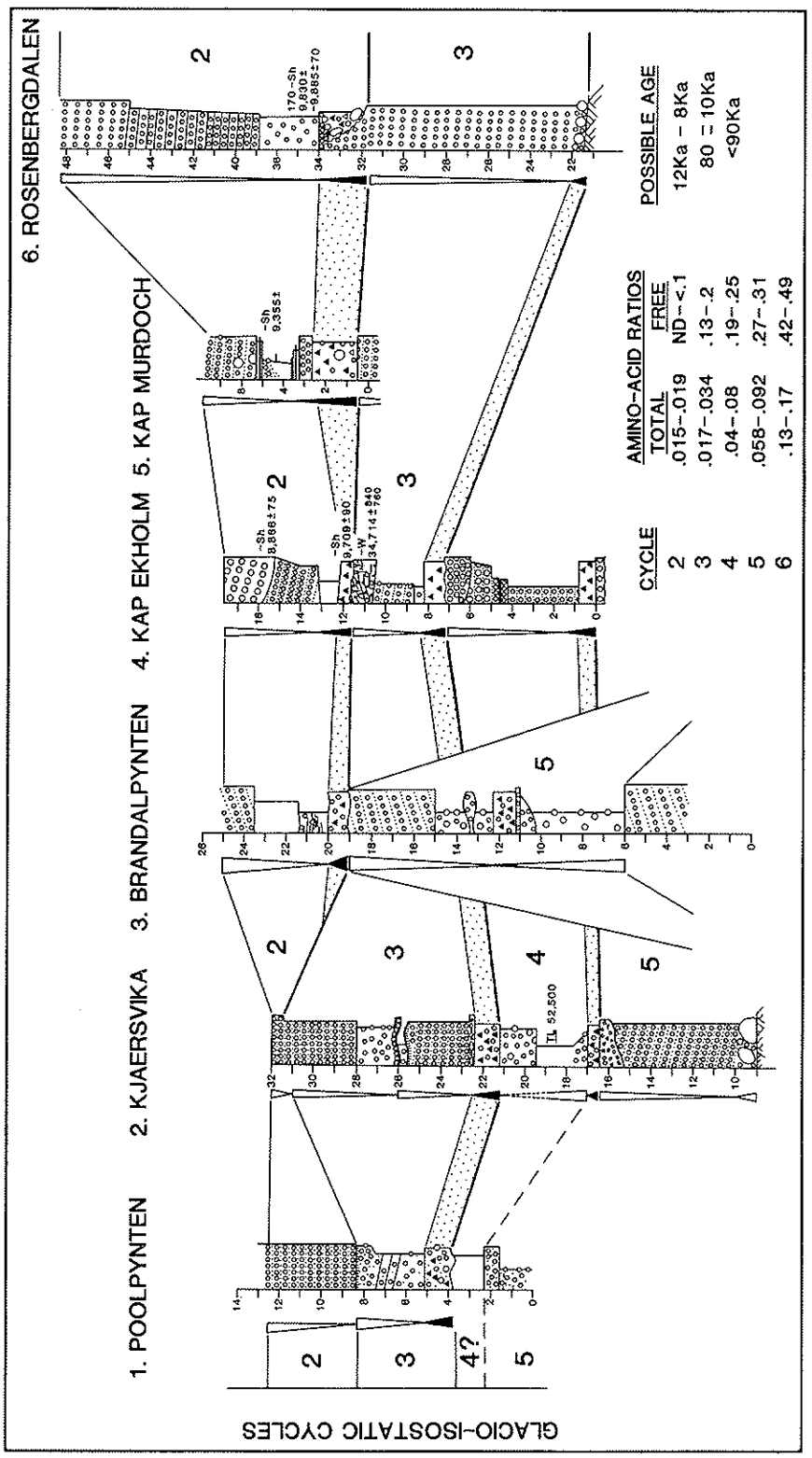

Fig. 27. Sedimentary logs through sequences of superimposed glacio-isostatic facies cycles. Individual cycles are numbered 2 to 5. Cycle 2 is of Late-Weichselian age and cycle 3 probably of Early Weichselian age. The locations of the sections 1–6 are shown in Figs 25 & 26.

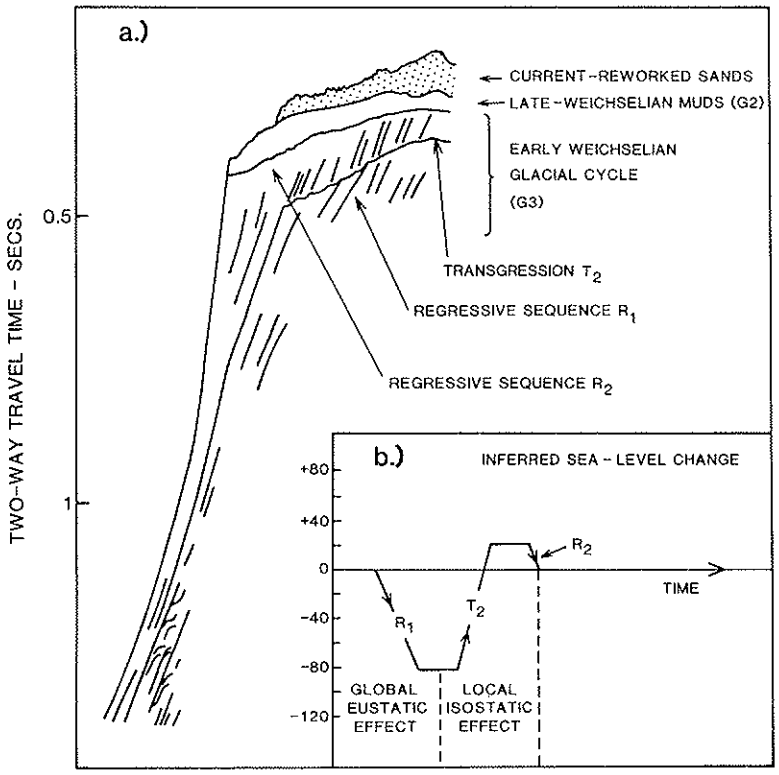

Fig. 28. (a) Detail of interpretation an of air-gun record across the trough mouth fan at the western extremity of Kongsfjordrenna (Fig. 11). (b) Interpretation of the structure in (a) in terms of sea level change through a whole glacial cycle.

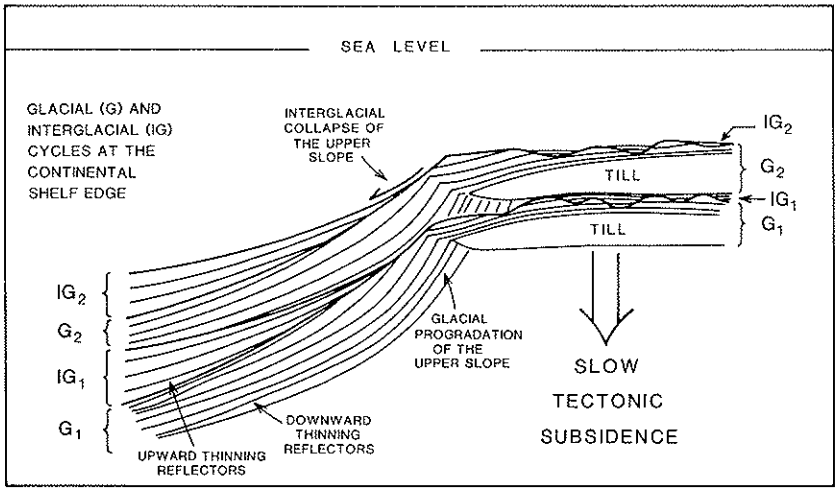

Fig. 29. Idealized structure of a shelf edge and upper slope in which glacier expansion to the shelf edge produces upper slope progradation, and phases of glacier retreat permit collapse of the upper slope and build-up of sediments lower on the slope. Tectonic subsidence permits a vertical sequence to build up which would otherwise be removed by energetic shelf processes.

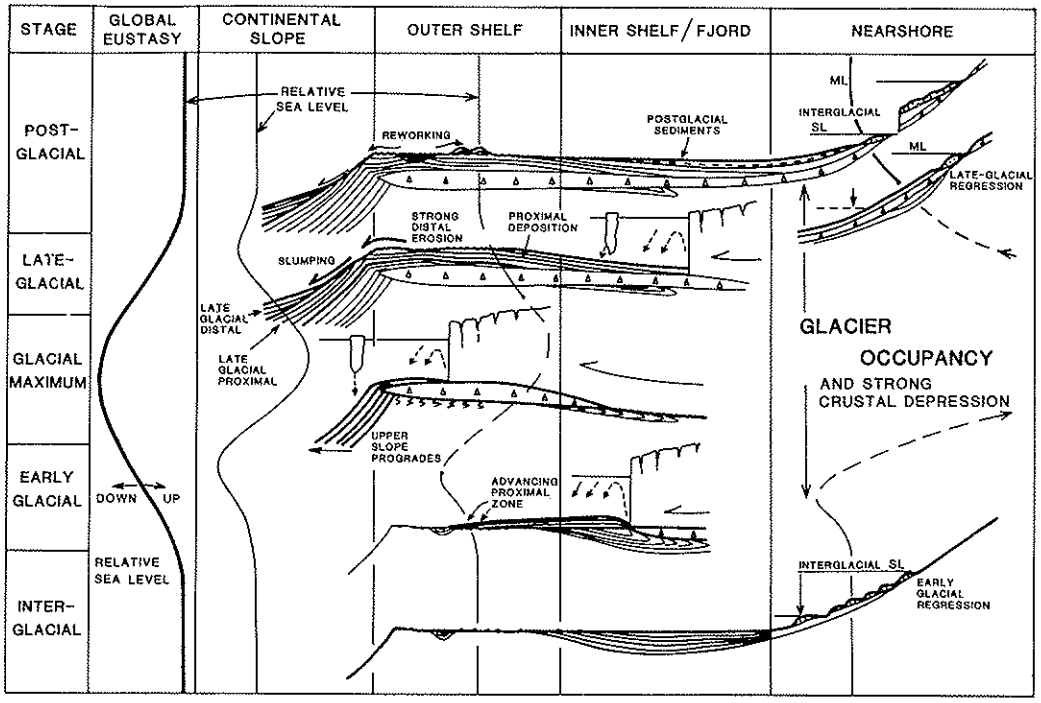

Fig. 30. A model of glacimarine architecture in space and time showing the building blocks of glacimarine facies architecture in different continental margin locations which accumulate through a whole glacial cycle. The relative sea level changes appropriate to each zone are shown.

shores of the Irish Sea and on the North Sea coast of England the last 10 000 years have seen a sea level rise from about −40 to −50 m bsl. On the northeast coast of Ireland (McCabe *et al.* 1986; McCabe & Eyles 1988) a marine limit up to +100 m asl lies above uplifted glacimarine sequences which in turn overlie tills, demonstrating an isostatically dominated high sea level immediately after deglaciation, followed by sea level regression. These patterns fit well with an ice sheet whose deglaciation leads global eustasy. The initial sea level fall from a high marine limit represents the early decay of the isostatic component and the later sea level rise represents the global eustatic rise. On the northeast coast of England the late-glacial marine limit is probably near or below sea level, reflecting the southeast axis of the Late Devensian British Ice Sheet which loaded the northern Irish Sea more than eastern England. Nonetheless, it shows a pattern of sea level change similar to that of the northern Irish Sea and reflecting early deglaciation. Flandrian sea levels appear to show a continuous rise (Tooley 1978), from −40 m at about 10 ka B.P. suggesting a low glacial sea level and a eustatically dominated postglacial transgression. However, just off the coast of northeast England, the Late Devensian glacimarine St Abb's beds occur in water depths of 40 m. implying that relative sea level during deglaciation was at least as high as −10 m. Thus, late-glacial sea level must have been isostatically-dominated, regressing from about −10 m at deglaciation to at least −40 m at 10 ka, followed by a eustatically dominated transgression up to modern sea level by about 4 ka.

c. Multiple glaciation. Figure 27 shows a series of sections across the Spitsbergen archipelago which contain evidence of pre-Late Weichselian glacial events. Some are represented by complete glacio-isostatic facies cycles, but some by only parts of cycles, either because of subglacial erosion (e.g. Brandalpynten, Rosenbergdalen, beneath cycle-2 till) or littoral and sub-littoral erosion (e.g. Kjaersvika, top of cycle 5), or because the magnitude and period of ice sheet loading was inadequate to produce strong crustal depression and sufficient marine submergence to ensure deposition of a glacimarine mud component (e.g. Poolpynten, base of cycle 2). Sites 1 and 2 in Fig. 27 lie beyond the limit of

Late Weichselian glaciation. However, they underwent a limited amount of glacio-isostatic submergence, with marine limits of 13 m and 32 m respectively. Water depth at the transgression maximum at these sites was not, however, great enough to ensure preservation of a mud sequence above sea level. The sites would be represented by a position at about 1100 km in Fig. 22.

A magnificent example of preservation of glacio-isostatic facies sequences is demonstrated by Eiriksson (1981) from the Late Cenozoic of Tjørnes, Iceland. In the volcanic area of northern Iceland, sites which emerge above sea level are likely to be covered by lava in a geologically-short time after emergence. The area has been subject to frequent glaciation during the Late Cenozoic, most of which have been large enough to produce a major isostatic effect and typical glacio-isostatic facies sequences. Shortly after emergence, the coarse littoral sediments are overlain by lavas, which are resistant to glacier erosion in the succeeding glacial phase, thus helping to preserve underlying cycles. The sequence is of remarkable thickness because of local tectonic subsidence. The mean net rate of sedimentation has clearly been equivalent to the subsidence rate as isostatically-dominated cycles recur throughout a sequence of at least 600 m. This is true however in many areas of tectonic subsidence which are glacier fed. The rate of sediment discharge is always more than adequate to keep pace with subsidence, but the sediment accumulation rate is restrained by erosional processes in the zone of strong bottom currents near to sea level, with the consequence that the net deposition rate is tectonically controlled.

Effects of multiple glaciation are also seen in marine-limit relationships. In areas of relative tectonic stability, the highest marine-limits beyond the extent of recent glaciation will be coeval with the extent of the largest and longest phase of glacier expansion. Figs 26 and 27 show such relationships in western Spitsbergen where, beyond the limits of Late Weichselian glaciation, a marine limit associated with a more extensive Mid-Early Weichselian glacial episode (cycle 3) lies between 30 and 60 m above the Late Weichselian marine limit.

Facies architecture on the continental shelf-edge and slope

The architecture of shelf-edge and upper continental slope sequences reflects the form of the continental margin, the current regime, sea level and sediment supply. Along the Spitsbergen continental margin, and glacimarine margins such as those of east Greenland and southern Iceland, there is a considerable contrast between the mouths of glaciated troughs and the shelf edge adjacent to intervening shallow banks. Within the trough mouth fans of western Spitsbergen topset units tend to comprise successive couplets of till and glacimarine mud as a result of glacier expansion to or near to the shelf edge. At least three such couplets have developed at the mouth of Isfjordrenna (Fig. 13a). Evidence from the west coast of Spitsbergen (Salvigsen 1977; Boulton *et al.* 1982; Miller 1982) suggests that the last phase of glacier expansion beyond the west coast cannot have been younger than early Weichselian (75–100 ka). If, as some have suggested (Andrews 1974; Mørner 1977; Boulton *et al.* 1982), high latitude glacial maxima develop during the early parts of glacial periods, it is possible that each couplet represents similar early phases of separate Late Pleistocene 100 ka glacial cycles, and that their stacking one above the other is facilitated by passive thermal subsidence of the Spitsbergen continental margin, which carries older units below an erosional base level prior to accumulation of succeeding units. Extrapolated subsidence rates derived from the evidence of Myhre & Eldholm (1988) of about 20 m/100 ka are compatible with this suggestion.

The detailed seismic stratigraphy of these shelf edge couplets may reveal the pattern of sea level change through a whole glacial cycle in a way which has not been reported elsewhere. Figure 28a shows a seismic section across the mouth of the Kongsfjordrenna fan. If we initially assume that at some fixed depth below sea level there is a transition from erosion to deposition, then the offlapping reflectors of R_1 would reflect a relative sea level fall of about 80 m (Fig. 28b). The subsequent upward shift of the point of progradation would reflect relative sea level rise of about 100 m, partly coeval with emplacement of the till unit by a glacier which advanced to the shelf edge. The subsequent offlapping reflectors of R_2 would reflect a relative sea fall to an approximately modern level. This sequence may represent the complete glacial cycle of sea level change, similar to that shown in Fig. 17–5b. The R_1 sequence would reflect slow eustatic sea level fall, associated with shelf progradation, initially because of stronger erosion in shallower shelf waters and subsequently because of the approach of the glacier. The lagged isostatic response to glacier loading then causes a rapid relative sea level rise. The progradation in the R_2 sequence may reflect a nearby source

of glacial sediment, whilst the offlap would represent relative sea level fall as a result of deglaciation and crustal rebound. The height of the transgression prior to final sea level fall would define the marine limit. The early Weichselian glacier extension beyond the modern coastline (cycle 3 in Fig. 27), which may have been the glacial phase in which the uppermost glacial couplet at the shelf edge was deposited, is associated with a marine limit of abou' 70 m at the coastline (Fig. 26), extrapolating to a marine limit of 50–60 m at the shelf edge. This compares with a marine limit inferred from seismic stratigraphy of 20 m. However, we would expect the amplitude of relative sea level change associated with ice sheet expansion to be overestimated from evidence of shelf-edge sediments, as increased sediment discharges will tend to reduce the critical erosion/deposition depth, and more energetic circulation to increase this during phases of reduced glacier extent.

There is a strong contrast between sediment architecture in the trough-mouth sediment wedges and on the flanking shallow banks. Seismic textures in the sediment forming the bank topsets are typical of those which we associate with till. Major 'till' masses are separated by relatively well defined reflecting surfaces, rather than the thick inter-till units found in the trough-mouth wedges. It is suggested that this reflects the relative shallowness of these banks which, during period of glacier retreat, are subject to strong bottom-current and/or iceberg scour which either remove glacimarine mud units produced during glacial maxima or homogenize them in iceberg turbates (Barnes & Rearic 1985). Similar bank-trough contrasts are found at the shelf edge of southeast Iceland (Boulton *et al.* 1988). The most recent sediment package on the upper and middle continental slope of West Spitsbergen shows internal reflectors and bounding surfaces which diverge with depth (Fig. 13b), demonstrating that recent sedimentation rates progressively increase from the shelf break to the middle slope (basement ridges on the lower slope complicate the pattern of sedimentation in deeper waters; Fig. 13a). Major slumped masses within this unit and other signs of instability on the upper slope (Fig. 14), suggest that the downward increase in net sedimentation rate predominantly reflects slumping of pre-existing upper slope sediments. This unit overlies the lateral equivalent on the upper continental slope of the uppermost glacial couplet, which is developed as a wedge of sediment at the shelf break, and which reflects substantial building-out of the shelf edge. It becomes thinner in deeper water. On the basis of these relationships, I suggest that, during the last extension of glaciers to the shelf edge, large contemporary sediment discharges over the shelf edge led to building out of the upper continental slope. On glacier withdrawal and the re-establishment of a S–N coastal current dispersing sediment to the north, the shelf edge was relatively starved of a primary sediment supply and underwent a net mass loss by slumping, to produce thick sediment accumulations on the middle and lower slope. I suggest that this may be a repetitive pattern of evolution of the edges of many glaciated shelves (Fig. 29) although even the Spitsbergen shelf shows complications such as the deflection of sediment dispersal pathways towards the northwestern shelf edge during the present interglaciation, and consequent modern progradation of the shelf edge there.

Summary

Figure 30 summarizes the way in which the individual facies associations, which are the building blocks of the sedimentary architecture, are emplaced in time and space during a complete glacial cycle.

Some of the fieldwork reported here was done in association with J. Jarvis, N. Chroston, C.T. Baldwin, J.D. Peacock and G.H. Miller; their contributions are gratefully acknowledged. Results are also derived from the SAFE programme, and from cruises of the *G A Reay* (1986) and *Tydeman* (1988). Collaboration in these with J.P.M. Syvitski, J. Jarvis, J.J.M. van der Meer, G. Postma, R. Schüttenhelm and C. Mesdag is gratefully acknowledged. Much of the work was generously supported by NERC and the Royal Society of London. An anonymous referee's helpful comments are also acknowledged.

References

Alley, R.B., Blankenship, D.D., Bentley, C.R. & Rooney, S.T. 1987. Till beneath ice stream B.3. Till deformation: evidence and implications. *Journal of Geophysical Research*, **92**, 8903–8912.

Anderson, J.B., Brake, C.F. & Myers, N.C. 1984. Sedimentation on the Ross Sea Continental Shelf, Antarctica. *Marine Geology*, **57**, 295–333.

Andrews, J.T. 1974. Cainozoic glaciations and crustal movements of the Arctic. *In*: Ives, J.D. & Barry, R.G. (eds.) *Arctic and Alpine Environments*. Methuen, London, 277–317.

Barnes, P.W. & Rearic, D.M. 1985. Rates of sediment disruption by sea ice as determined from characteristics of dated ice gouges created since 1975 on the inner shelf of the Beaufort Sea, Alaska. *United States Geological Survey Open File Report 85–473.*

BIRNIE, R.V. 1977. A snow-bank push mechanism for the formation of some 'annual' moraine ridges. *Journal of Glaciology*, **18**, 77–85.

BOULTON, G.S. 1982. Subglacial processes and the development of glacial bedforms. *In*: DAVIDSON-ARNOTT, R., NICKLING, W., & FAHEY, D.D. (eds.) *Glacial, Glacio-fluvial and Glacio-lacustrine Systems*. Geo Books, Norwich.

—— 1986. Push moraines and glacier-contact fans in marine and terrestrial environments. *Sedimentology*, **33**, 667–698.

—— 1987. A theory of drumlin formation by subglacial deformation. *In*: ROSE, J. & MENZIE, J. (eds) *Drumlins*, Balkema, Rotterdam, 25–81.

——, BALDWIN, C.T., PEACOCK, J.D., MCCABE, A.M., MILLER, G., JARVIS, J., HORSFIELD, B., WORSLEY, P., EYLES, N., CHROSTON, P.N., DAY, T.E., GIBBARD, P., HARE, P.E. & VAN BRANN, V. 1982. A glacioisostatic facies model and amino acid stratigraphy for late Quaternary events in Spitsbergen and the Arctic. *Nature*, **298**, 437–441.

—— & HINDMARSH, R.C.A 1987. Sediment deformation beneath glaciers: rheology and geological consequences. *Journal of Geophysical Research*, **92**, 9059–9082.

—— & JONES, A.S. 1979. Stability of temperate ice sheets resting on beds of deformable sediment. *Journal of Glaciology*, **24**, 29–43.

——, SMITH, G.D., JONES, A.S. & NEWSOME, J. 1985. Glacial geology and glaciology of the last mid-latitude ice sheets. *Journal of the Geological Society of London*, **142**, 447–474.

——, SMITH, G.D. & MORLAND, L.W. 1984. The reconstruction of former ice sheets and their mass balance characteristics using a non-linearly viscous flow model. *Journal of Glaciology*, **30**, 140–152.

——, THORS, K. & JARVIS, J. 1988. Dispersal of glacially-derived sediment over part of the continental shelf of south Iceland. *Marine Geology*, **83**, 193–223.

—— & VAN DER MEER, J.J.M. (eds) 1989. *Report on an expedition to Spitsbergen in 1984 to study glaciotectonic phenomena*. University of Amsterdam.

——, VAN DER MEER, J.J.M. & CAMERAAT, E. 1985. Side-entry systems in fiords: inputs to the fiords from their margins. *In*: SYVITSKI, J.P.M. & BLAKENEY, C. (eds) *Sedimentology of Arctic Fiords Experiment*, vol. 2 Canadian Data Report of Hydrography and Oceans Sciences, **28**, 121–126.

COOPE, G.R. & BROPHY, J.A. 1972. Late-glacial environmental changes indicated by a coleopteran succession from North Wales. *Boreas*, **1**, 97–142.

DALE, J.E., AITKEN, A.E., GILBERT, R. & RISK, M.J. 1989. Macrofauna of Canadian Arctic Fjords. *Marine Geology*, **85**, 331–358.

DE GEER, G. 1910. Guide de l'excursion au Spitzberg. Excursion A1. *XIe Congres Geologigue Internationale*, Stockholm.

EIRIKSSON, J. 1981. Lithostratigraphy of the upper Tjörnes sequence, North Iceland: the Breidavik Group. *Acta Naturalia Islandica*, **29**, 1–37.

ELVERHØI, A. 1984. Glaciogenic and associated marine sediments in the Weddell Sea, fjords of Spitsbergen and the Barents Sea: a review. *Marine Geology*, **57**, 53–88.

——, LØNNE, Ö. & SELAND, R. 1983. Glacimarine sedimentation in a modern fjord environment, Spitsbergen. *Polar Research*, **1**, 127–149.

—— & ROALDSET, E. 1983. Glacimarine sediments and suspended particulate matter, Weddell Sea, Antarctica. *Polar Research*, **1**, 1–21.

FARROW, G.E., SYVITSKI, J.P.M. & TUNNICLIFFE, V. 1983. Suspended particulate loading on the macrobenthos in a highly turbid fjord; Knight Inlet, British Columbia. *In*: GORDON, D.E. (ed.) *Turbid Water Symposium. Canadian Journal of Fisheries and Aquatic Sciences*, 132–152.

GRIPP, K. 1929. Glaciologische und Geologische Ergebnisse der Hamburgischen Spitzbergen-Expedition 1927. *Abhandlung-Naturwissenschaftlicher Verein Zu Hamburg*, **XXII**, 147–249.

HINDMARSH, R.C.A., MORLAND, L.W., BOULTON, G.S. & HUTTER, K. 1987. The unsteady flow of ice sheets: a parabolic problem with two moving boundaries. *Geophysical and Astrophysical Fluid Dynamics*, **93**, 183–223.

HOPPE, G. 1948. Isrecessionen från Norrbottens Kustland i belysning av de glaciala formelementen. *Geographica*, **20**.

HOSKIN, C.M., BURRELL, D.C. and FREITAG, G.R. 1978. Suspended sediment dynamics in Blue Fjord, Western Prince William Sound, Alaska. *Estuarine and Coastal Marine Science*, 7, 1–16.

JACOBS, S.S. 1989. Marine controls on modern sedimentation on the Antarctic continental shelf. *Marine Geology*, **85**, 121–153.

KING, L.H. & FADER, G. 1986. Wisconsinan glaciation of the continental shelf – southeast Atlantic Canada. *Geological Survey of Canada, Bulletin*, **363**.

——, ROKOENGEN, K & GUNLEIKSRUD, T. 1987. Quaternary seismostratigraphy of the Mid-Norwegian Shelf, 65°–67°31N – A till tongue stratigraphy. *Institutt for Kontinentals okkelndersökelser publication*, **114**.

LAMPLUGH, G.W. 1911. On the shelly moraine of the Sefström glacier and other Spitsbergen phenomena illustrative of British glacial conditions. *Proceedings of the Yorkshire Geological Society*, **17**, 216–241.

LUNDQUIST, J. 1986. Stratigraphy of the central area of the Scandinavian glaciation. *Quaternary Science Reviews*, **5**, 269–292.

MANGERUD, J., BOLSTAD, M., ELGERSMA, A., HELLIKSEN, D., LANDVIK, J.Yl, LYCKE, K., LØNNE, I., SALVIGSEN, O., SANDAHL, T. & SEJRUP, H.P. 1987. The Late Weichselian glacial maximum in Western Svalbard. *Polar Research*, **5**, 275–278.

MCCABE, A.M. & EYLES, N. 1988. Sedimentology of an ice-contact glacimarine delta, Carey Valley, Northern Ireland. *Sedimentary Geology*, **59**, 1–14.

——, HAYNES, J.R. & MACMILLAN, N.F. 1986. Late-

Pleistocene tidewater glaciers and glacimarine sequences from north County Mayo, Republic of Ireland. *Journal of Quaternary Science*, **1**, 73–84.

MILLER, G.H. 1982. Quaternary depositional episodes, western Spitsbergen, Norway: aminostratigraphy and glacial history. *Arctic and Alpine Research*, **24**, 321–340.

MIX, A.C. & RUDDIMAN, W.F. 1985. Structure and timing of the last deglaciation: oxygen-isotope evidence. *Quaternary Science Reviews*, **4**, 59–108.

MOIGN, A. 1965. Contribution à l'étude littorale et sous-marine de la Baie du Roi, Spitsberg. *Cahiers oceanographiques*, **8**, 453–563.

MORLAND, L.W., SMITH, G.D. & BOULTON, G.S. 1984. Basal sliding relations deduced from ice sheet data. *Journal of Glaciology*, **30**, 131–139.

MYHRE, A.M. & ELDHOLM, O. 1988. The western Svalbard margin (74°–80°N). *Marine and Petroleum Geology*, **5**, 134–156.

MØRNER, N.A. 1977. Southward displacement of the distribution of glaciation during the three maxima of the last ice age. *Journal of Glaciology*, **18**, 305–308.

OERLEMANS, J. & VAN DER VEEN, C.J. 1984. *Ice Sheets and Climate*. Reidel, Dordrecht.

ORHEIM, O. & ELVERHØI, A. 1981. Model for submarine glacial deposition. *Annals of Glaciology*, **2**, 123–128.

PELTIER, W.R., FARRELL, W.E. & CLARK, J.A. 1978. Glacial isostasy and relative sea level: a global finite element model. *Tectonophysics*, **50**, 81–110.

POWELL, R.D. 1981. A model for sedimentation by tidewater glaciers. *Annals of Glaciology*, **2**, 129–134.

—— & COWAN, E.A. 1986. Depositional processes at McBride Inlet and Riggs glacier. *In*: ANDERSON, P.J., GOLDTHWAIT, R.P. & MCKENZIE, G.D. (eds) Observed Processes of Glacial Deposition in Glacier Bay, Alaska. *Ohio State University, Institute of Polar Studies, Miscellaneous Publications*, **256**, 140–156.

SALVIGSEN, O. 1977. Radiocarbon datings and the extension of the Weichselian ice-sheet in Svalbard. *Norsk Polarinstitutt Aarbok*, **1976**, 209–242.

SOLHEIM, A. & PFIRMAN, S.L. 1985. Sea floor morphology outside a grounded, surging glacier: Bråsvellbreen, Svalbard. *Marine Geology*, **65**, 127–143.

SOLHEIM, A., RUSSWURN, L., ELVERHØI, A. & NEYLAND BERG, M. 1990. Glacial geomorphic features in the northern Barents Sea: direct evidence for grounded ice and implications for the pattern of deglaciation and late glacial sedimentation. *In*: DOWDESWELL, J.A. & SCOURSE, A.D. (eds), *Glacimarine Environments: Processes and Sediments*. Geological Society, London, Special Publication, **53**, 253–268.

SYVITSKI, J.P.M. 1987. Proximal prodelta investigations at two arctic deltas: Itirbilung and Cambridge Fiords, Baffin Island. *Geological Survey of Canada Open File*, **1589**, ch. 6.

—— 1989. On the deposition of sediment within glacier-influenced fjords: oceanographic controls. *Marine Geology*, **85**, 301–329.

——, BURRELL, D.C. & SKEI, J.M. 1983. *Fjords: Processes and products*. Springer, New York.

TOOLEY, M.J. 1978. *Sea level fluctuations in North-West England during the Flandrian Stage*, Clarendon, Oxford.

TURCOTTE, D.L. & SCHUBERT, G. 1982. *Geodynamics. Applications of continuum physics to geological problems*. Wiley, New York.

VORREN, T.O., LEBESBYE, K., ANDREASSEN, K. & LARSSEN, K-B. 1989. *Marine Geology*, **85**, 251–272.

WALCOTT, R.I. 1973. Structure of the earth from glacio-isostatic rebound. *Annual Review of Earth and Planetary Sciences*, **1**, 15–37.

WEERTMAN, J. 1972. General theory of water flow at the base of a glacier or ice sheet. *Reviews of Geophysics and Space Physics*, **10**, 287–333.